A concept to evaluate dynamic daylight glare

Efthymia Eirini Tsianaka

Master thesis in Energy-efficient and Environmental Buildings
Faculty of Engineering | Lund University

Lund University

Lund University, with eight faculties and a number of research centers and specialized institutes, is the largest establishment for research and higher education in Scandinavia. The main part of the University is situated in the small city of Lund which has about 112 000 inhabitants. A number of departments for research and education are, however, located in Malmö. Lund University was founded in 1666 and has today a total staff of 6 000 employees and 47 000 students attending 280 degree programmes and 2 300 subject courses offered by 63 departments.

Master Programme in Energy-efficient and Environmental Building Design

This international programme provides knowledge, skills and competencies within the area of energy-efficient and environmental building design in cold climates. The goal is to train highly skilled professionals, who will significantly contribute to and influence the design, building or renovation of energy-efficient buildings, taking into consideration the architecture and environment, the inhabitants' behaviour and needs, their health and comfort as well as the overall economy.

The degree project is the final part of the master programme leading to a Master of Science (120 credits) in Energy-efficient and Environmental Buildings.

Examiner: Marie-Claude Dubois (Energy and Building Design)

Supervisor: Niko Gentile (Energy and Building Design)

Keywords: glare, daylight, zonal, long-term, adaptation possibility, TPG, STG, directional glare, weighting system, dynamic, visual comfort, fenestration system

Thesis: EEBD - # / 18

Abstract

Visual comfort is becoming a significant concern of contemporary building design. The increased interest for utilizing daylight in buildings sets the question for visual comfort. One of the serious challenges in the whole process is the identification and reduction of glare issues. The objective of this study is to propose the concept of an evaluation methodology of the discomfort glare in a dynamic and zonal way, using existing glare indices. In more detail, the method considers different observer's positions and gaze directions, as well as observer's adaptation possibility in terms of head rotation and glare duration. In order to account for glare extended in space and duration, the method currently uses an arbitrary weighting system. The method is first applied in a point-in-time analysis. Later, the thesis shows the application of the proposed methodology in a hypothetical library room with different shading devices using the existing glare metrics of DGP, DGI and DGPs. With the foreseen increase in computational power and given that an evidence-based weighting system would replace the proposed one, the thesis shows that the proposed method may help at the early design stage of interior design of spaces, e.g. by guiding in the placement of desks.

Acknowledgments

The author would like to express her great appreciation and gratitude to her supervisor Niko Gentile, for his enthusiastic encouragement, guidance and valuable suggestions during the development of this thesis. Furthermore, the author is thankful to the staff of Inform Design AB for the constructive and beneficial discussions that we had during the first stage of the thesis. Moreover, the author would like to thank Nathaniel Jones and Mostapha Sadeghipour Roudsari for answering questions regarding Accelerad and Honeybee plug in compatibility.

Table of content

Symbols

G: generic glare index [-]

L_s: luminance of glare source [cd/m^2]

L_b: background luminance [cd/m^2]

ω_s: the solid angle subtended by the glare source [steradians]

Ω_s: the solid angle altered to include the effect of the observer's position related to the source [steradians]

E_v: vertical illuminance at the eye [lx]

E_d: direct vertical illuminance at the eye [lx]

P: position index [-]

φ: weighting value for directional gaze [-]

t: percentage of time duration without imperceptible glare [%]

ω_{tot}: total studied period of time [h]

Abbreviations

HDRI: High dynamic range imaging

BREEAM: Building Research Establishment Environmental Assessment Method

sDA: Spatial daylight autonomy

$ASE_{1000,250}$: Annual sunlight exposure

OF: Openness factor

T_{vis}: Visual transmittance

DGP_t: Threshold DGP for a critical glare situation

G_{dir}: directional glare

TPG: Total Point glare

STG: Space-Time glare

BSDF: Bidirectional scattering distribution function

Definitions

Non-uniform glare source: Glare source with non-uniform luminance distribution (i.e. window)

Uniform glare source: Glare source with uniform luminance distribution (i.e. artificial lighting)

Position Index: The position of the glare source in the field of view

Vertical Illuminance: Illuminance measured at the eye level, specifically on a plane perpendicular to the line of sight

Background luminance: The average luminance of the surrounding (background) with the luminance of the glare source being excluded.

"Don't ask me about this building or that one, don't look at what I do, see what I see."

- Luis Barragan

1 Introduction

1.1 Aim

The main objective of the thesis is to propose a conceptual framework for dynamic and zonal glare assessment, based on existing glare indices.

The conceptual framework consists of repeated glare analysis for different observer positions and different times. The information is combined in order to obtain an overall glare risk evaluation for a certain area. Consequently, the method should support the late-stage of the design process, namely the proper positioning of indoor partitions or furniture arrangement.

1.2 Background

Existing glare indexes refer to specific condition for *a point in time* and *a point in space with a direction of sight*. This implies that they are mostly useful to predict glare at a very late design stage, that is when the fenestration system is already designed, and all the laying out of the space is decided (e.g. desk position, partitions). The equations describing glare probability estimate glare according to the parameter that they are based on[1] (Jakubiec and Reinhart, 2016), ignoring any possible change in user's position and his gaze during the occupation time. Therefore, the search for a new criterion comparing the existing indices and including all the aforementioned factors is needed.

On the other hand, moving outside the research field, current policies generally propose simple methods accounting for glare[2]. These methods can be based on components performance (BREEAM), or simple climate-based grid illuminance simulations throughout the year (LEED). They are used at an early design stage since they implicitly refer to an extended zone inside the space and a wide time span, which are supposedly glare-free. In other words, the policies refer to glare as *zonal* and *dynamic*. However, the methods used by policies, presented further below in *Literature Review*, are not very reliable predictors of glare.

1.3 Literature Review

1.3.1 Glare metrics

The main reason for designing and improving indoor spatial and environmental quality has been the insurance of physical and psychological human well-being. Daylight analysis and utilization, being directly connected to those factors (Andersen, 2015), comprise an important aspect of the designing process. During the past years, research in the daylight field has been intensively growing. Visual comfort and specifically prediction models for discomfort glare, though, are still largely debated in the scientific community.

[1] e.g. contrast, extreme brightness, dim situations.

[2] Excluding the future European Standard EN17037.

According to Wienold and Christoffersen (2006), most of the proposed discomfort glare formulas are based on a common general form (eq.1).

$$G = \left(\frac{L_s^e \cdot \omega_s^f}{L_b^g \cdot f(\psi)} \right) \quad [-] \tag{1}$$

where, e, f, g: weighting exponents, and ψ: displacement angle

As a general methodological approach, the development of a glare prediction formula involves observations, where individual subjective responses are correlated to some kind of photometric measurements, and an empirical model is therefore derived. The experimental conditions determine the conditions in which the derived glare prediction formula is applicable. As a consequence, to date, there is not yet a universal metric that would accurately predict discomfort glare for every possible case (Tzempelikos, 2017).

For example, the Visual Comfort Probability (VCP) proposed by Guth and Luckiesh (1949), was the first glare metric that was based on psychological assessments of glare issues (eq.2)[3]. The VCP equation was derived from experiments with small uniform fluorescent lamps and thus could not provide accurate results when large uniform or non-uniform glare sources were tested (Hirning, 2014). According to Suk *et al.* (2017), VCP reported excessed risk for glare, when was examined under daylight conditions, confirming the initial thoughts.

$$\boldsymbol{VCP = \frac{100}{\sqrt{2\pi}} \cdot \int_{-\infty}^{6.374-1.3227\, ln(DGR)} \left(e^{-t^2/2} \cdot dt \right)} \quad [-] \tag{2}$$

where, DGR: Discomfort Glare Rating.

On the contrary, the British Research Station Glare Index (BRS or BGI), introduced by Hopkinson and Petherbridge (1950), took into account glare sources from large surfaces with increased brightness (eq.3). BGI was the first glare metric to consider the reflectance from the surrounding space. However, when used to predict indoor glare under daylight conditions, the results differed from those provided by the observers in the field. The reason was that the empirically emerged formula derived under artificial lighting conditions, all glare sources were accounted as one condensed parameter and the possible adaptation was not included (Robinson *et al.*, 1962; Iwata *et al.*, 1990; Carlucci *et al.*, 2015).

$$BGI = 10\, log_{10}\, 0.478 \cdot \sum_{i=1}^{n} \frac{L_s^{1.6} \cdot \omega_s^{0.8}}{L_b \cdot P^{1.6}} \quad [-] \tag{3}$$

In an attempt for those limitations to be minimized, Einhorn (1969) presented the CIE Glare Index (CGI) (eq.4). The CGI equation, although emerged from experiments with uniform glare sources, included a specific parameter for adaptation, using the glare source illuminance (E_d) and the background illuminance (E_i) (Einhorn, 1979). Iwata *et al.* (1990) researched the accuracy of the CGI metric under an artificial glare source representing the size of a window (screen), and concluded that CGI and BRS overestimates glare. However, according to

[3] The entire equation of VCP metric can be found in APPENDIX A.1.

Jakubiec and Reinhart (2012), though, CGI could be considered as an appropriate metric for testing the worst-case scenario due to glare overestimation.

$$CGI = 8\,log_{10}\,2 \cdot \frac{\left(1 + \frac{E_d}{500}\right)}{E_d + E_i} \cdot \sum_{i=1}^{n} \frac{L_s^2 \cdot \omega_s}{P^2} \quad [-] \tag{4}$$

The first index evaluating glare under non-uniform glare was the Cornell or Daylight Glare Index (DGI) developed by Hopkinson (1972) (eq.5).

$$DGI = 10\,log_{10} 0.48 \cdot \sum_{i=1}^{n} \frac{L_s^{1.6} \cdot \Omega_s}{L_b + 0.07\omega_s^{0.5} L_s} \quad [-] \tag{5}$$

The DGI formula was based on the BRS and CGI metric, and it was derived from experiments with artificial light placed behind a diffusive fabric (Bellia *et al.*, 2008; Piccolo and Simone, 2009). According to Jakubiec and Reinhart (2012), DGI fails to predict glare when the sun is directly visible or if the scenario is brightly illuminated. In addition, recent evaluation studies with subjects found that DGI may underestimate glare (Suk *et al.*, 2017).

VCP, BGI and CGI approaches were later combined into the Unified Glare Rating (UGR) system by CIE (1995) (Reinhart and Wienold, 2011) (eq.6). In the UGR, the adaptation parameter introduced by CGI was replaced by background luminance on a vertical plane (L_b). UGR was initially developed by means of experiments with uniform glare sources and thus could not be accurately applied to daylight conditions. A later edited version of the UGR equation was specifically generated to cover cases with non-uniform glare sources or specular reflectance, but, according to CIE (2002), emerged after hypothesis and estimations and thus would not provide reliable results (Eble-Hankins and Waters, 2009). UGR is widely used today to evaluate glare from electric light sources.

Recently, a modified version of the UGR formula, the Unified Glare Probability (UGP), was proposed for open plan space analysis in tropical climates (Hirning *et al.*, 2017; Lim *et al.*, 2017)[4].

$$UGR = 8\,log_{10}\,\frac{0.25}{L_b} \cdot \sum_{i=1}^{n} \frac{L_s^2 \cdot \omega_s}{P^2} \quad [-] \tag{6}$$

Another glare index specifically developed for daylight is the Predictive Glare Sensation Vote (PGSV), presented by Tokura *et al.* (1996) (eq.7). The PGSV was derived after experiments carried out under a fixed artificial light source situated behind different opening sizes covered with fabric. Compared to the UGR, the PGSV equation connected the background luminance with the size of the glare source, in order to account more accurately for the adaptation. However, according to Iwata and Tokura (1998), PGSV may underestimate glare.

[4] The UGP formula can be found in APPENDIX A.1.

$$PGSV = 3.2\,log\,L_s - 0.64\,log\,\omega + (0.79\,log\,\omega - 0.61)\,log\,L_b - 8.2 \quad [-] \qquad (7)$$

Today, the most widely used daylight glare metric is the Daylight Glare Probability (DGP) introduced by Wienold and Christoffersen (2006) (eq. 8).

$$DGP = 5.87 \cdot 10^{-5} \cdot E_v + 9.18 \cdot 10^{-2}\,log_{10}\left(1 + \left(\sum_{i=1}^{n} \frac{L_{s,i}^2 \cdot \omega_{s,i}}{E_v^{1.87} P_i^2}\right)\right) + 0.16 \quad [-] \quad (8)$$

The DGP was developed following test on 74 subjects in different daylight scenarios, for a total of 349 cases. The subjective response was correlated to the luminance distribution at the window and the vertical illuminance at the eye level (E_v). The DGP equation includes the Guth Position Index (Pi)[5], which indicates the position of the observer (Luckiesh and Guth, 1949; Iwata and Tokura, 1997). When DGP, CGI, VCP and UGR were tested under daylight conditions and compared to in situ evaluation, the resulting data indicated that DGP outperformed, having the lowest risk for inaccurate results (Jakubiec and Reinhart, 2012). The reliability of DGP upheld its success in daylighting practice. Yet DGP has some limitations which are worth mentioning.

Firstly, although derived from a relatively big dataset, the DGP model may not accurately predict daylight glare for some daylight scenarios. For example, DGP results in foreseeable outcomes with extreme or barely noticeable glare conditions, but it fails in intermediate conditions (Suk *et al.*, 2017).

Secondly, when the sun rays reach directly the task area, the DGP predictions are less precise, since the increased luminance is considered as another glare source (Van Den Wymelenberg *et al.*, 2010). Konstantzos and Tzempelikos (2017) proposed the modified Daylight Glare Probability (DGP_{mod}) to overcome such limitation (eq. 9). The DGP_{mod} formula was developed after experiments with roller shades of different openness factor and visual transmissivity. However, DGP_{mod} could only be used with specific spatial conditions and not be generalized. According to Konstantzos and Tzempelikos (2017), also, when fabrics with high openness factor were implemented, a high divergence between the resulting data and the real conditions emerged, indicating extreme glare risk which was not observed in reality.

$$DGP_{mod} = 8.40 \cdot 10^{-5} \cdot E_v + 11.97 \cdot 10^{-2}\,log\left(1 + \sum_{i=1}^{n} \frac{L_{s,i}^2 \cdot \omega_{s,i}}{E_v^{2.12} p_i^2}\right) + 0.16 \quad [-] \quad (9)$$

Finally, a drawback of the DGP metric is that its calculation requires higher computational capacity in comparison to other existing metrics.

[5] The different equations for the description of the P_i can be found in APPENDIX A.1.

In order to reduce the simulation time, Wienold (2007) proposed the simplified Daylight Glare Probability (DGPs) (eq.10). The DGPs requires only the knowledge of E_v and it excludes effect of direct glare sources; consequently it can only be used when there were no specular reflectances in the scene and the sun is not in the field of view (Wienold, 2007; Carlucci *et al.*, 2015). Howerver, by measuring only the E_v rather than accounting also for the L_b could potentially misrepresent the glare risk (Chan et al., 2015).

Similarly, the enhanced simplified Daylight Glare Probability (eDGPs) is another "light" version of the DGP, which can be used if the scene is lacking of specular reflectances (Wienold, 2009) (eq.11).

$$DGPs = 6.22 \cdot 10^{-5} \cdot E_v + 0.184 \quad [-] \tag{10}$$

$$eDGPs = c_1 \cdot E_v + c_2 \, log_{10}\left(1 + \left(\sum_{i=1}^{n} \frac{L_{s,i}^2 \cdot \omega_{s,i}}{E_v^{1.87} P_i^2}\right)\right) + c_3 \quad [-] \tag{11}$$

1.3.2 Policies framework

Some standards, regulations and certification mechanisms dedicate sections regarding daylight evaluation. In most cases, glare is evaluated in a very simple way.

For example, the Building Research Establishment Environmental Assessment Method (BREEAM, 2017) mentions a method for glare control that focuses on the form of the building and the designed shading system (automatic or manual). BREEAM does not specify a glare prediction metric; rather it states that glare control, through shading systems, would not be necessary when the sun would not face the façade directly or under cloudy conditions. In other terms, BREEAM, implies that the main cause for glare problems derives from direct sun beams and the visible sun. Any possible glare arising from excessive contrast is excluded.

Likewise, the Leadership in Energy and Environmental Design rating system (LEED, 2018) requires, as a first step, the implementation of an occupant-control or semi-automatic shading system. Following, based on annual simulation with the shading system being excluded, the spatial Daylight Autonomy ($sDA_{300/50\%}$) is recommended to be at least[6] 55%, while the Annual Sunlight Exposure ($ASE_{1000,250}$) below 10%. Alternatively, according to LEED, the illuminance levels should not exceed the 3000lx. Although, sDA is considered as a reliable zonal glare measurement (IES, 2012; Atzeri *et al.*, 2016), ASE, sDA and illuminance levels could be accounted only as preliminary glare indicators and not as actual glare metrics.

A more specific method for glare estimation is to be presented in the European Standard on Daylight of Buildings, currently under development (prEN 17037, 2016). According to the index of the standard drafts, the DGP metric should be used. The current draft recommends DGP to be at most 0.45 or 0.35 for minimum or maximum glare protection, while it could exceed those values but only for maximum 5% during the occupied time.

[6] 55% for 2 credits and 75% for 3 credits in an often-used area.

1.4 Thesis questions

The short review on glare metrics showed that current glare metrics require high computing capacities and they are mostly of use during an advanced design stage. The short review on policies showed that other zonal and dynamic predictors of glare are easy to be used, but they lack validation.

Given the increasing computational capacity, the main investigated question of this thesis is:

- How can existing glare metrics be combined in order to propose a zonal and dynamic evaluation of glare for a defined space at an early design stage?

Therefore, the thesis does not aim to create a new glare metric, rather it proposes a conceptual framework to use the existing metrics in an earlier design stage. The concept is entirely based on mathematical elaborations and lacks validation with human subjects.

1.5 Hypotheses - Limitations

This thesis is divided in two parts. The first, which is the core of the thesis, is the proposal of a concept to evaluate dynamic and zonal glare. The second is an example of application of the concept. Each of the two parts has a number of limitations.

For the first part:

- The concept is based only on reasonable assumptions. A validation with real observers was not conducted.

- The reasonable assumptions include some arbitrary weighting systems. The weighting systems come as a proposal and they should be modified or validated by means of field studies.

- In definitive, the conceptual framework should serve as inspiration and it does not aim to provide conclusive statements.

For the second part:

- The materials were assumed to be diffusive without roughness or specularity, as the focus of the thesis did not include a sensitivity analysis of the materials.

- For a reduced computational time, no surrounding buildings were added to the tested geometry.

- The method and all the stated metrics, according to Piccolo and Simone (2009), do not account for the spectral light distribution.

- There was a lack of existing validation and extended research regarding the accuracy of the current BSDF method evaluation (Tzempelikos and Chan, 2016). The provided

BSDF from the manufacturer and the occurring data used during the simulations of this thesis, were affected by this limitation.

- The number of the tested shading elements occurred based on the computational time and the thesis time restriction. An increased number of tested elements (e.g. openness factor for the roller shades and reflectance for the venetian blinds) could result in different relationships between the data.

- Only one orientation, towards South, was investigated. Other orientations, such as West, would indicate different results.

- The glare prediction through a fish eye view and DGP, according to Kim et al. (2009), provided accurate results only 30° above and below the line of view.

- The relationship between the glare sensation and the characteristics of the view through a bare window was not accounted in this thesis (Tuaycharoen and Tregenza, 2007). Likewise, the effect of a shading system in the view out clarity through metrics, such as View Clarity Index (VCI), and the relationship to the glare sensation was not considered in this thesis (Konstantzos *et al.*, 2015).

- The possibility of other factors influencing glare sensation , such as fatigue, food intake, caffeine ingestion, degree of eye opening or visual neuron excitability were not taken into account (Bargary *et al.*, 2015; Yamin Garreton *et al.*, 2015; Altomonte *et al.*, 2016).

2 Methodology

2.1 Conceptual framework

The conceptual framework includes three main steps:

1. Check different glare metrics for the same scene
2. Repeat Step 1 for the same scene with different observer positions and gaze directions
3. Include in Step 2 an adaptation possibility for the observer, i.e. the observer may decide to slightly move the gaze to avoid glare, and the observer may accept glare if the overall glare duration does not exceed a reference time.

The observer's adaptation is most critical part of the conceptual framework since it needs validation with real observers. For the scope of this thesis, the assumptions and weighting systems were partially inspired by the so-called "adaptive zone", presented by Jakubiec and Reinhart (2012) and further explored by Jakubiec in his PhD dissertation (Jakubiec, 2014).

2.1.1 Investigated glare metrics

The indoor luminous scene would often account for direct beam illuminance and reflections. In such situation, glare prediction is improved when more than a single glare metric is examined, see Jakubiec and Reinhart (2016). Three glare indices were implemented in the presented method:

- **DGP**, for an overall assessment considering both brightness and contrast
- **DGPs**, to focus on brightness rather than contrast
- **DGI**, to focus on contrast rather than brightness

Indeed, DGP considers most parameters that affect the glare sensation (Jakubiec and Reinhart, 2012). The first part of the DGP formula predicts discomfort glare from brightly illuminated scenes due to Ev, while the second part estimates the contrast parameter or adaptation (Wienold and Christoffersen, 2006) (Figure 1). DGPs equation focuses more on brightness, as it derives from the first part of the DGP equation. DGPs could provide a good correlation with DGP in case of sun patches being present on the work plane and in general on the indoor planes (Konstantzos et al., 2015). DGI focuses more on the contrast as comprises an older version of the second part of the DGP metric[7].

The luminance map generated for the DGP analysis can be reused for the next two glare indexes, so adding DGPs and DGI add information on glare with little to no cost in terms of computational time. The three indexes have different threshold, see Table 1.

[7] The reason that other glare metrics were not used can be found in APPENDIX A.1.

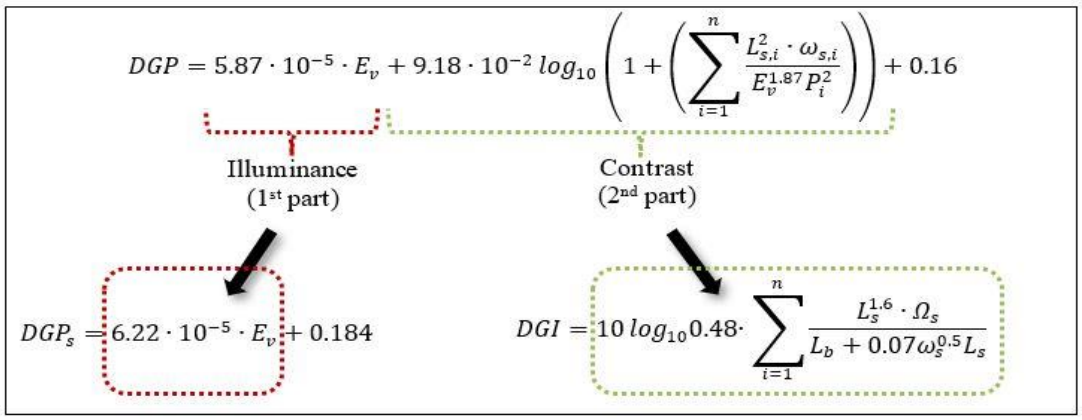

Figure 1: Diagram presenting the correlation between the investigated glare metrics.

Table 1: Threshold for the glare indexes (from literature).

Glare magnitude	**DGP**	**DGPs**	**DGI[8]**
A. Imperceptible	< 0.35	< 0.35	< 18
B. Perceptible	0.35-0.40	0.35-0.40	18 – 24
C. Disturbing	0.41-0.45	0.40-0.45	24 – 31
D. Intolerable	> 0.45	> 0.45	> 31

2.1.2 Position and Gaze direction

The glare indexes should be now calculated for every time step at different observers' position and gaze directions. Theoretically, there is an infinite number of combinations between the observers' position and gaze direction. In order to save computational time, the combinations should be reduced to only the necessary ones. Defining exactly the necessary ones is difficult, but knowing that the glare risk decreases when the glare source is distant from the visual centre (Tokura *et al.*, 1996; Jakubiec and Reinhart, 2011), it is reasonable to focus on areas potentially closer to glare sources (e.g. sun patches) and where the luminosity may change more often.

The conceptual framework envisages an initial analysis aiming at identifying areas where direct sunlight falls. In such areas, the density of simulated observer's positions is higher. The analysis is grid-based and requires little computational effort.

For each of these observer's positions, the centre of vision is assumed central, integral to the head of the observer, and moved -15° below the standard line of view, to simulate the potential sitting view focused on a screen. The observer's head can rotate by 180° (Figure 2).

[8] The specific DGI rating was based on McNeil and Burrell study (2016), in order to be compared with DGP and DGPs.

For the case study, which is later illustrated, such analysis was conducted with the eye position set at 1.2m above the floor, resembling an observer sitting in front of a computer screen. Based on this analysis, 12 different points were chosen (Figure 2). As mentioned, the grid is denser where direct sunlight hours are higher.

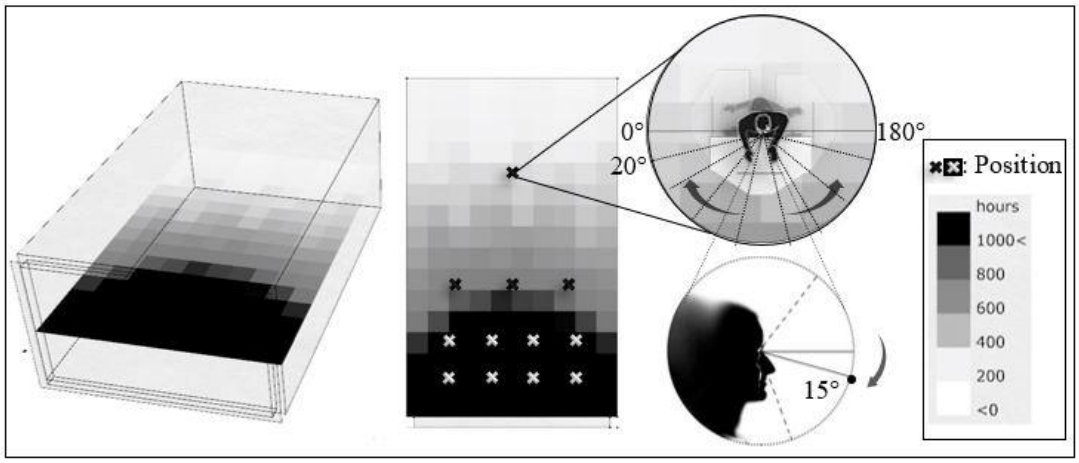

Figure 2: Picture showing the total hours of direct sun based on annual analysis, the emerged observer's positions and the rotation of the gaze.

2.1.3 Adaptation Possibility

At this stage, the method would provide a number of glare predictions, one for each sitting position and gaze direction, and all at a defined point-in-time. However, Jakubiec and Reinhart (2012) showed that the observer may slightly rotate to avoid glare (the aforementioned "adaptive zone"), while it seems that the observer may accept glare if the glare duration does not exceed a reference time (prEN 17037, 2016). Thus, for the data processing, a weighting system for *adaptation possibility* was created. The adaptation can be:

- in terms of **head rotation**
- in terms of **glare duration**

The weighting system adopted for both case of *adaptation possibility* was based on reasoned assumptions for a computer-based task. Therefore, the weighting system is proposed as a concept, while the value of weights need in-depth investigation and validation by means of *ad hoc* research with real individuals.

2.1.3.1 Adaptation possibility in terms of head rotation

According to literature, glare sensation increases when the glare source is closer to the visual centre (Jakubiec and Reinhart, 2011). Thus, glare at neutral head position should be weighted more. The exact weight to assign is an open question, but for the sake of demonstration in this thesis, it was assumed to be an exponentiation of 2 starting from the extreme rotation positions (0° and 180° degrees) (Figure 3). In practice, if the neutral position shows glare, the generic glare index is multiplied by 32. However, if the 40 degrees position shows glare, then the generic glare index is multiplied only by 8. If the glare is still present even after a rotation (for

example to 60°), the glare index at this position is multiplied by 16 (eq. 12), see example in Figure 4.

$$adaptation\ possibility\ in\ terms\ of\ head\ rotation = \varphi \cdot G_{dir} \quad [-] \qquad (12)$$

- G_{dir}: the glare results based on different head positions (in terms of head rotation), named as *directional Glare.*
- φ: weighting factor assumed to be an exponentiation of 2 (arbitrary).

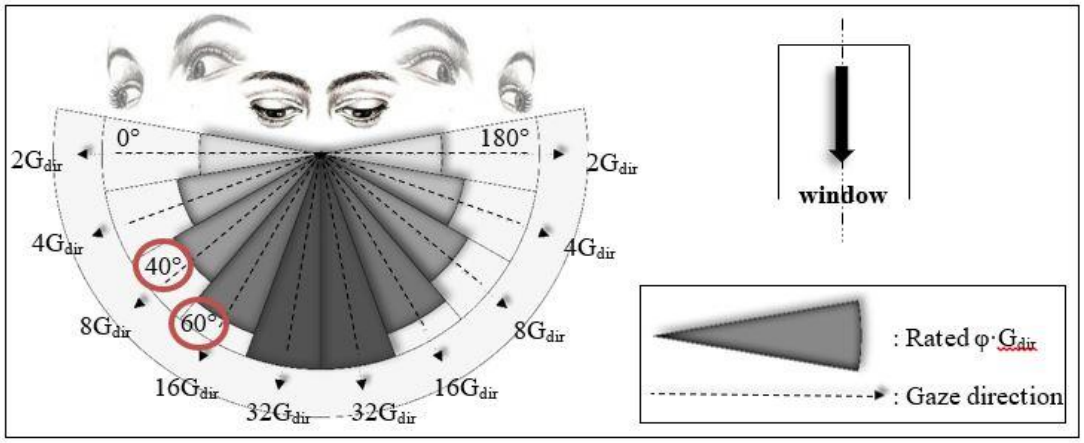

Figure 3: Diagram showing the calculation of the different G_{dir} and the glare credits for the weighting system.

	A	B	C	D
1		Position -1-		
2	ϕ	Head rotation	DGP (10:00)	Results
3	2	-90	0.252756	0.505512
4	4	-70	0.284171	1.136684
5	8	-50	0.311682	2.493456
6	16	-30	0.33826	5.41216
7	32	-10	0.346818	11.098176
8	32	10	0.34881	11.16192
9	16	30	0.348735	5.57976
10	8	50	0.332526	2.660208
11	4	70	0.320259	1.281036
12	2	90	0.274821	0.549642
13				

Figure 4: Explanatory diagram of the adaptation possibility in terms of head rotation for one observer position at 10:00.

2.1.3.2 Adaptation possibility in terms of glare duration

The study is inspired by the preliminary version of the European Standard on Daylight of Buildings (prEN 17037, 2016). The standard sets duration thresholds for the values of DGP during usage time, with the scope of evaluating shading devices. Even though this standard does not evaluate the severity of prolonged glare independently from the shading devices, the thresholds proposed in the prEN 17037 (2016) are, at the best of the author's knowledge, among the few proposals dealing with the issue of prolonged glare. Therefore, the method presented in this thesis proposes a weighting system inspired by the preliminary version of the standard, which is shown in Table 2.

Table 2: Weighting system for evaluating severity of glare prolonged in time.

Glare index ranges		**Threshold during usage time (from prEN 17037, 2016)**	**GlareCredit**	
DGP/DGPs	**DGI**		**GlareCredit$_{initial}$**[9]	**GlareCredit$_{changed}$**
< 0.35	< 18	-	**1**	**1**
0.35 – 0.40	18 – 24	5%	**2**	**1**
0.41 – 0.45	25 – 31	5%	**3**	**2**
> 0.45	> 31	5%	**4**	**3**

In practice, the GlareCredit is assigned based on whether the glare occurred for more or less than 5 % of the usage time (eq. 13, eq.14). In mathematical terms:

If glare duration ≥ 5% then,

$$adaptation\ possibility\ in\ terms\ of\ glare\ duration = \boldsymbol{GlareCredit_{initial}} \cdot G_{dir} \quad [-] \quad (13)$$

else,

$$adaptation\ possibility\ in\ terms\ of\ glare\ duration = \boldsymbol{GlareCredit_{changed}} \cdot G_{dir} \quad [-] \quad (14)$$

- *GlareCredit$_{initial}$:* the weighting factor in case the glare duration is more than 5%
- *GlareCredit$_{changed}$:* the weighting factor in case the glare duration is less than 5%
- *GlareCredit:* the weighting factor for the adaptation possibility in terms of glare duration (GlareCredit$_{initial}$ or GlareCredit$_{changed}$)

Figure 5 works as an explanatory diagram of the aforementioned weighting system for the glare duration. The simulated glare values of two observer positions with different head rotations per hour are presented.

[9] The values for the credits were arbitrary, based on the increased severity of the glare risk.

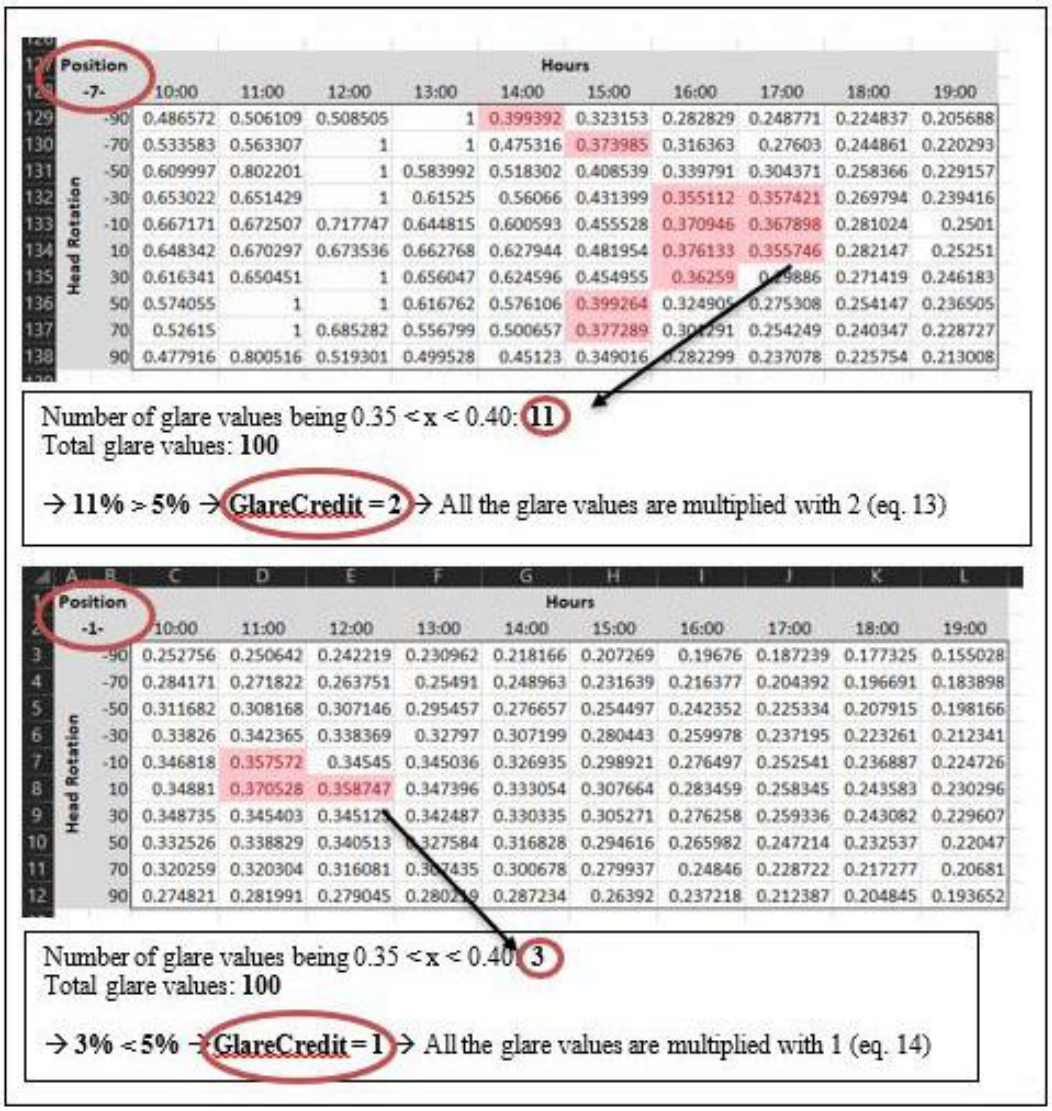

Figure 5: Explanatory diagram of the adaptation possibility in terms of glare duration for two observer positions (glare values of DGP).

The concepts of adaptation possibility in terms of head rotation and glare duration may be merged together (eq.15).

$$\boldsymbol{AdaptationPossibility} = \boldsymbol{\varphi} \cdot \boldsymbol{G_{dir}} \cdot \boldsymbol{GlareCredit} \quad [-] \qquad (15)$$

In order to extract one glare value per observer position (taking into account the adaptation possibility), two equations were developed based on different kind of analyses (presented also in Figure 6):

1. point-in-time analysis → *Total Point Glare* equation (**TPG**)
2. during a period of time analysis → *Space-Time Glare* equation (**STG**)

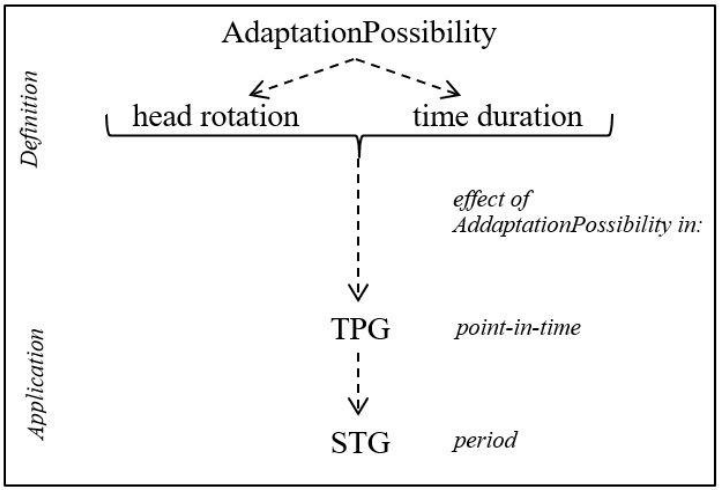

Figure 6: Explanatory diagram of the correlation between AdaptationPossibility and TPG-STG.

2.1.3.3 TPG

The *Total Point Glare* (TPG) represents the normalization of the *adaptation possibility* (eq. 15) with respect to the worst-case scenario. Therefore, TPG defines the severity of glare (in percentage) at one observer position, but for multiple gaze directions in a point-in-time (eq.16).

$$\boldsymbol{TPG} = \left(\frac{\sum_{i=1}^{n} AdaptationPossibility_i}{TPG_{max}}\right) \cdot 100 \quad [\%] \tag{16}$$

- *n:* total number of gaze directions (G_{dir}) in a certain position
- *i:* each of the different gaze directions starting from 0º to 180º, with 20º steps (see Figure 3)
- TPG_{max}*:* the maximum TPG, i.e. when all the directional gazes of a specific position would have **disturbing glare** per hour

$$TPG_{max} = GlareCredit \cdot \sum_{i=1}^{n} \varphi_i \cdot G_{dir,max} \quad [-] \tag{17}$$

- GlareCredit = 3 (weighting factor for disturbing glare) (see Table 1 and Table 2)
- $G_{dir,max}$= 0.45 (for DGP/DGPs) or $G_{dir,max}$ = 31/100 =0.31 (for DGI[10]).

[10] All the resulted DGI values were divided by 100 in order to be compared with DGP-DGPs as percentage of 100.

Once the normalization is performed, the method would require a target value for TGP, (TPG_{target}). Even in this case, in lack of field tests with individuals, the target was arbitrarily chosen as equal to **perceptible glare** for all directions.

$$TPG_{target} = GlareCredit \cdot \sum_{i=1}^{n} \varphi_i \cdot G_{dir,target} \quad [-] \tag{18}$$

Where

- GlareCredit = 2 (weighting factor for perceptible glare) (see Table 1 and Table 2)
- $G_{dir,target}$ = 0.35 (for DGP/DGP_s) or $G_{dir,target}$ =18/100 =0.18 (for DGI).

Using the aforementioned values, eq. 17 and eq. 18 will numerically become:

$$\overset{(17)}{\Longrightarrow} TPG_{max} = 3 \cdot (2 + 4 + 8 + 16 + 32 + \cdots + 2) \cdot G_{dir,max} = 3 \cdot 124 \cdot G_{dir,max} =$$

$$= 372 \cdot G_{dir,max} = \begin{cases} 372 \cdot 0.45 = 167.4, & for\ DGP\ or\ DGPs \\ 372 \cdot 0.31 = 115.32, & for\ DGI \end{cases}$$

$$\overset{(18)}{\Longrightarrow} TPG_{target} = 2 \cdot (2 + 4 + 8 + 16 + 32 + \cdots + 2) \cdot G_{dir,target} = 2 \cdot 124 \cdot DG_{dir,target}$$

$$= 248 \cdot G_{dir,max} = \begin{cases} 248 \cdot 0.35 = 86.8, & for\ DGP\ or\ DGPs \\ 248 \cdot 0.18 = 44.6, & for\ DGI \end{cases}$$

The following table summarizes the values for the TPG_{max} and the TPG_{target} (Table 3). In practice, TGP is considered acceptable when lower than 50% and 40 % of the maximum possible severity for DGP/DGPs and DGI respectively. It should be noted that the target percentages in Table 3 (last column) are different since DGP/DGPs and DGI scales (from imperceptible to intolerable glare) are different.

Table 3: The maximum and targeted TPG thresholds used for this thesis.

	TPG_{max} /-	**%**	**TPG_{target}** /-	**%**
DGP or DGPs	167.4	**100**	86.8	**50**
DGI	115.32	**100**	44.64	**40**

2.1.3.4 STG

The *Space-Time Glare* (STG) equation was created for the estimation of the total glare value on a certain observer position during a period. STG followed was a function of TPG and the studied time (eq.19), following the same normalization process as in TPG.

$$\boldsymbol{STG} = \left(\frac{\sum_{j=1}^{\omega_{tot}} (TPG_{y,j})}{STG_{max}} \right) \cdot 100 \quad [\%] \tag{19}$$

- ω_{tot}: the studied period of time
- j: the studied time step (here: per hour)
- y: the specific observer's position in space
- STG_{max}: The maximum STG per hour that was used as benchmark (100%).

STG_{max} was assumed to occur when TPG = TPG_{max}. In more details,

$$STG_{max} = TGP_{max} \cdot \omega_{tot} \quad [-] \tag{20}$$

STG_{target} was arbitrary chosen, being:

$$STG_{target} = TGP_{target} \cdot \omega_{tot} \quad [-] \tag{21}$$

Example: for DGP or DGPs,

$$\overset{(20)}{\Longrightarrow} STG_{max} = \begin{cases} 167.4 \cdot 7 = 1171.8, & if\ \omega = 7 \\ 167.4 \cdot 5 = 837, & if\ \omega = 5 \end{cases}$$

and,

$$\overset{(21)}{\Longrightarrow} STG_{target} = \begin{cases} 86.8 \cdot 7 = 607.6, & if\ \omega = 7 \\ 86.8 \cdot 5 = 434, & if\ \omega = 5 \end{cases}$$

The following table summarizes the values for the maximum and the target STG (Table 4)[11].

Table 4: The maximum and targeted STG thresholds used for this thesis.

	ω_{tot}	**STG_{max} /-**	**(%)**	**STG_{target} /-**	**(%)**
DGP or DGPs	7	1171.8	**100**	607.6	**50**
	5	837	**100**	434	**50**
DGI	7	807.24	**100**	312.48	**40**
	5	576.6	**100**	223.2	**40**

[11] APPENDIX B.1 for the analysis of the different studied days and the occuring period of time (ω).

2.2 Case study

The conceptual framework proposed in the previous section was later tested in a case study example. The case study includes a single geometry tested with four different shading devices. The test was run for three specific days throughout the year with one-hour time step, and one orientation that occurred after the climate analysis of the base case. The occupied hours of the library were 10am to 7pm, which is typical for libraries in Sweden.

The simulations of the base case were run using two sky models (extreme case scenarios):

- CIE clear sky with sun (testing mainly the influence of brightness and position of the glare source)
- CIE overcast sky (testing the contrast levels between indoor surfaces and window)

2.2.1 Studied geometry and material properties

The model proposed in this thesis was applied to a shoebox model. The model was a library room located in Stockholm, positioned three floors above the ground with an almost fully glazed façade (Figure 7)[12]. Also, the sill of the window was just above the floor, including any reflectances below the work plane, as the glare risk caused by a source below the line of sight was considered risky (Iwata and Tokura, 1997).

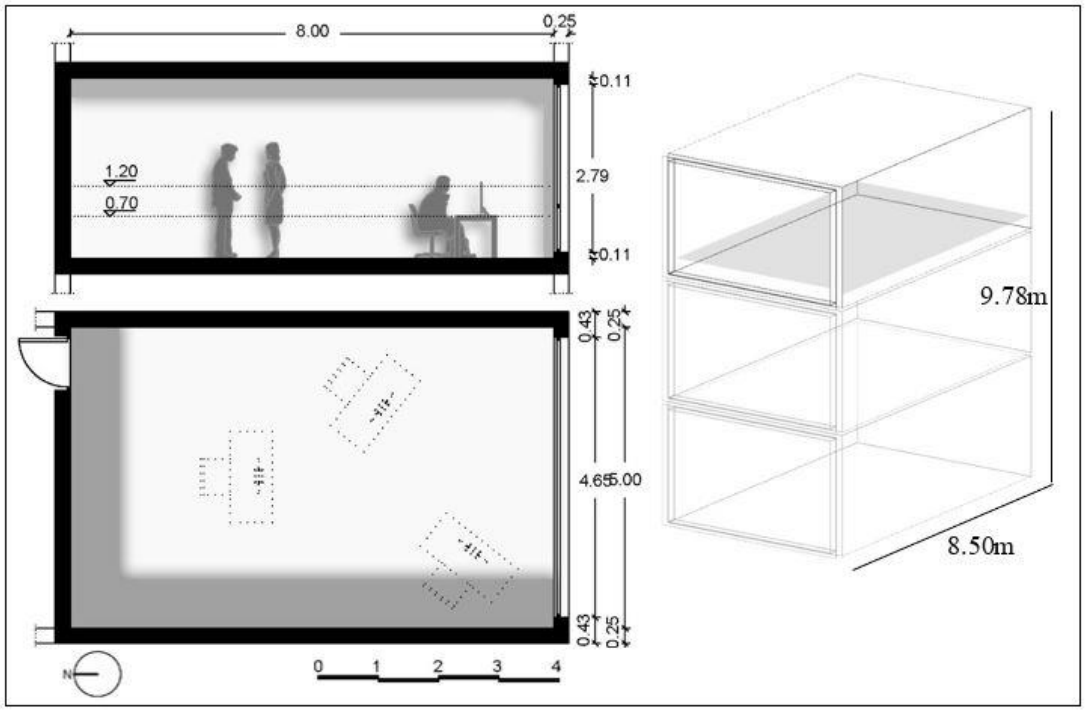

Figure 7: Plan, cross section and axonometric of the tested geometry.

[12] The shape of the room was chosen to be elongated (having the highest width lengthwise the façade) in order to present both dimed situations and daylit spaces.

The surface materials had properties as in Table 5. A computer screen was also simulated having one inner glow material (250 cd/m^2) and one outer glass. The rad parameters were constant throughout all the simulation process (APPENDIX A.2).

Table 5: The properties of the materials used.

Surface	**Reflectance**	**Transmission**
Interior Walls	0.5	
Ceiling	0.8	
Floor	0.25	
Sill	0.35	
Window, Double Pane-Clear		0.80
Screen glass, Single Pane		0.88

Four different shading systems were examined: two types of venetian blinds and two types of roller shade fabrics. All the shading systems would operate manually, having an On (window coverage: 3/4) and Off position. The venetian blinds would have a fixed slat angle of 40º as an effort to reduce the noise and enhance the focus conditions in the library. Their fixed slat angle and operating position was selected in a way so, that the percentage of the specular reflectances in the eye level to be as low as possible, while the illuminances in the rest area to fluctuate between 300lx and 3000lx according to LEED (2018) (Figure 8).

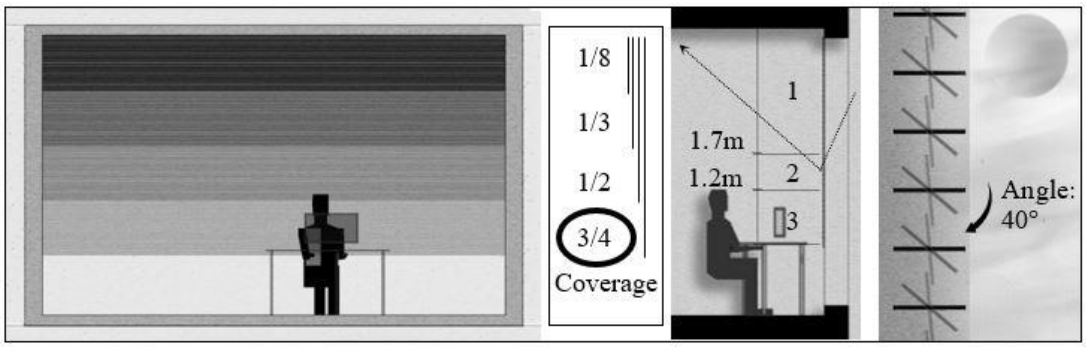

Figure 8: The tested window coverage and angles of the venetian blinds, as well as, the 3 areas investigated with forward raytracing.

Different properties of the implemented materials were tested, in order to evaluate their performance regarding daylight glare control throughout the reference zone (Table 6). The venetian blinds were varying in their slat reflectivity, while the fabric of the roller shades was varying in openness factor (OF) and visual transmittance (T_{vis}). The selection of the roller shades fabric was based on the research presented by Chan *et al.* (2015), where several fabric

properties were recommended based on the window orientation, the glazing visual transmittance and the building location.

Table 6: The properties of the tested materials.

Shading Systems	Reflectance	Roughness	Specularity	OF	T_{vis}	Color
1. Venetian Blinds	0.70	0.05	0.01			Grey
2. Venetian Blinds	0.50	0.05	0.01			Grey
3. Roller Shades[13]				0.30	10	White
4. Roller Shades				0.50	6	Charcoal

2.3 Software

During the simulation process, several programs were utilized. Initially, the model was created in Rhino3D and internalized in Grasshopper environment ('Rhinoceros 3D', 2018; 'Grasshopper 3D', 2018). A script was created with the use of Ladybug and Honeybee components, for the initial sun path investigation, the venetian blinds geometry examination and the final daylight analysis (Sadeghipour Roudsari and Pak, 2013). Separately, an investigation upon the roller shades properties was conducted in WINDOW software database. Later, the specific BSDF files, obtained by WINDOW, were evaluated in BSDFviewer and inserted in the script (Mitchell *et al.*, 2013; McNeil, 2016).

Radiance engine was incorporated in Honeybee for the dynamic visual comfort analysis, as well as the daylight autonomy (Fritz and Mcneil, 2018). As Honeybee plug in would provide information only for DGP and DGI, a special component for DGPs was created inside the Grasshopper environment, with the use of Python scripting (Piacentino, 2013). This component would provide the DGPs needed results, the vertical illuminance (E_v) and the direct vertical illuminance ($E_{v,dir}$), by analysing an HDRI image through Evalglare script in Radiance (McNeil, 2017). Finally, the resulted data were processed and visualized through Ladybug, and transferred through TT Toolbox (Core Studio, 2018) to Excel. The overall workflow is presented below (Figure 9).

[13] The pictures of the tested BSDF could be found in APPENDIX B.2.

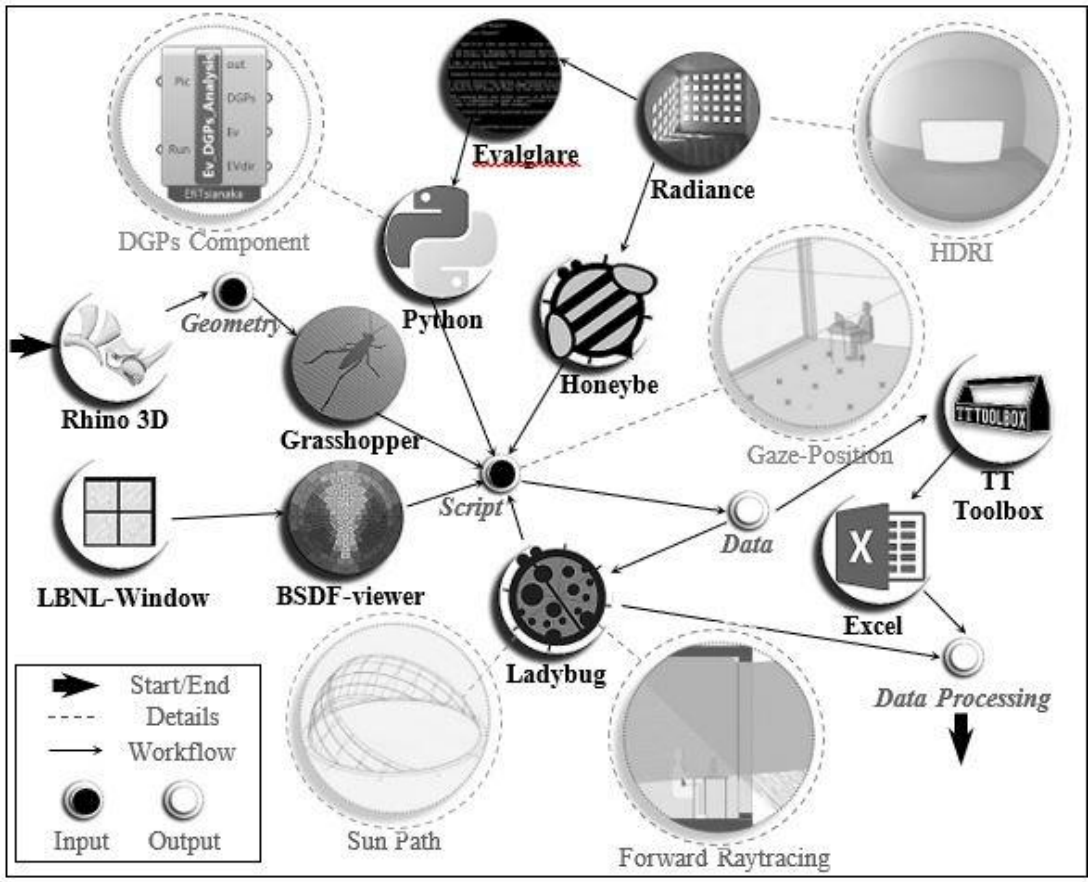

Figure 9: Diagram presenting the workflow.

Initially, in order to reduce the computational time, a new lighting analysis engine called Accelerad (Jones, 2017a) was used and compared to Radiance. It was found that both engines would provide the same results when the base case was studied, but Accelerad would significantly reduce the computational time by a third. This, mainly, occurred as GPU replaced the CPU, previously used for Radiance (Jones, 2017b). Unfortunately, some connectivity issues between Accelerad, which is currently in Beta mode, and Honeybee emerged. In addition, the current version of Accelerad does not support BSDF files, which were an important part of the case study. Thus, Radiance was preferred, eventually, over Accelerad.

3 Results

This chapter consisted by three sub-sections, with the last one being the most crucial of the thesis.

- *Base case analysis*
- *Shading systems*
- *Dynamic daylight glare evaluation*

The first and the second sections comprised the initial analysis, being done during the first steps of the thesis[14], in order to prepare the tested cases for the third section. This last section referred to the main topic of this thesis, i.e. the investigation of a method towards the dynamic daylight glare evaluation.

3.1 Dynamic Daylight Glare Evaluation

The following section was the most crucial of the thesis. The implementation of the *TPG* and *STG* in the method, as well as, their corresponding results were presented below.

3.1.1 TPG

The glare risk distribution in space per hour was examined with the use of TPG. The studied period was that of 21/12, which was taken as a worst-case scenario. The results of the TPG were presented as a space-temporal map, with the data being projected as a grid on the floor plan. More specifically, this space-temporal map was comprised by repeated rectangles (plan form) showing the different TPG values for each tested hour. The values of the three different glare metrics were presented in three columns, while the four tested shading systems were presented in four rows. Figure 10a and 10b were used as explanatory diagrams for the space-temporal map illustration.

[14] The initial analysis of the base case and the shading systems can be found in APPENDIX B.1 and B.2.

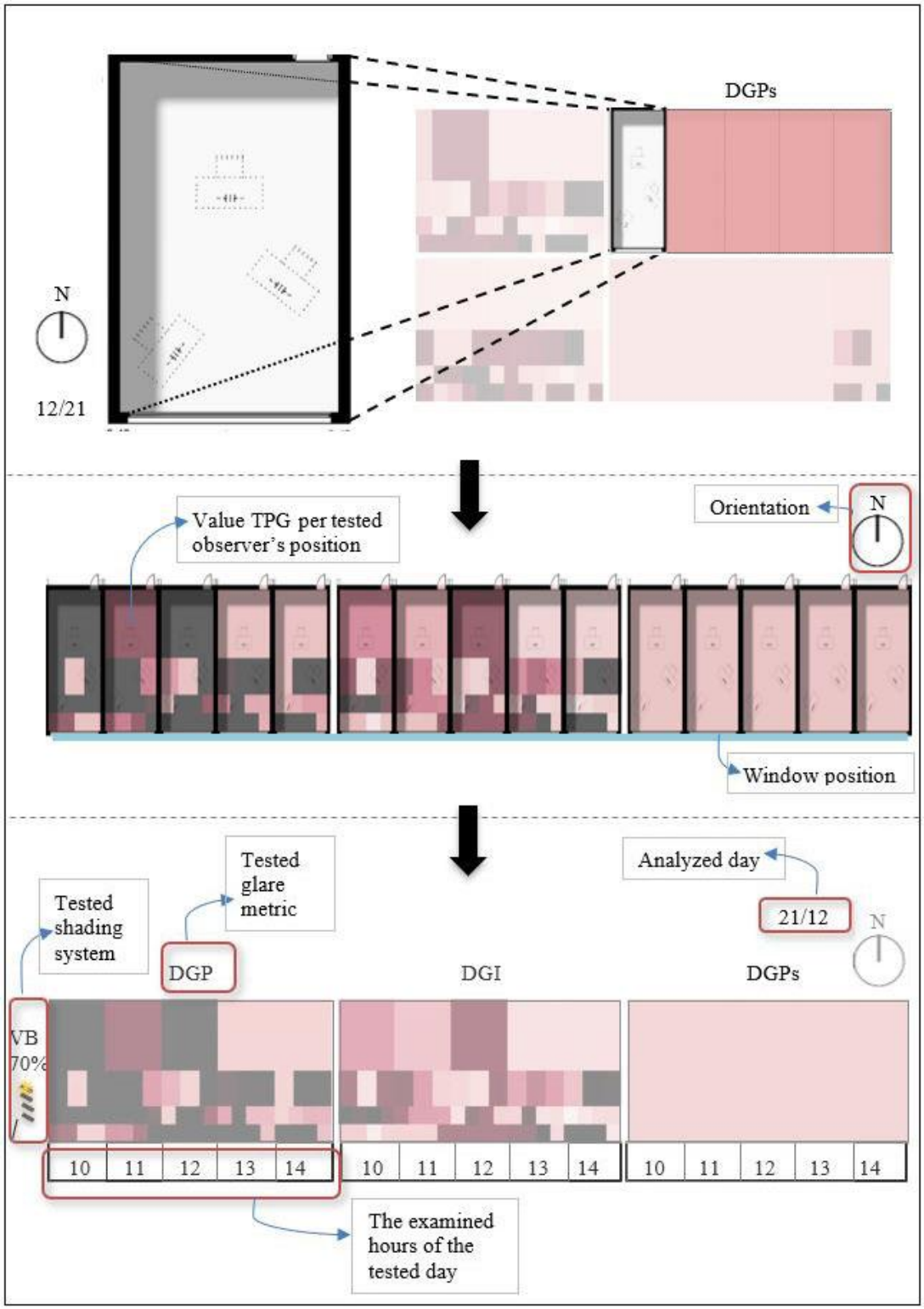

Figure 10a: Explanatory diagram of the space-time temporal map, used for the TPG illustration.

The values of the three different glare metrics (DGP, DGI, DGPs) were presented in three columns, while the four tested shading systems were shown in four rows (I: VB 70%, II: VB 50%, II: RS 7%, IV: RS 5%) (Figure10b).

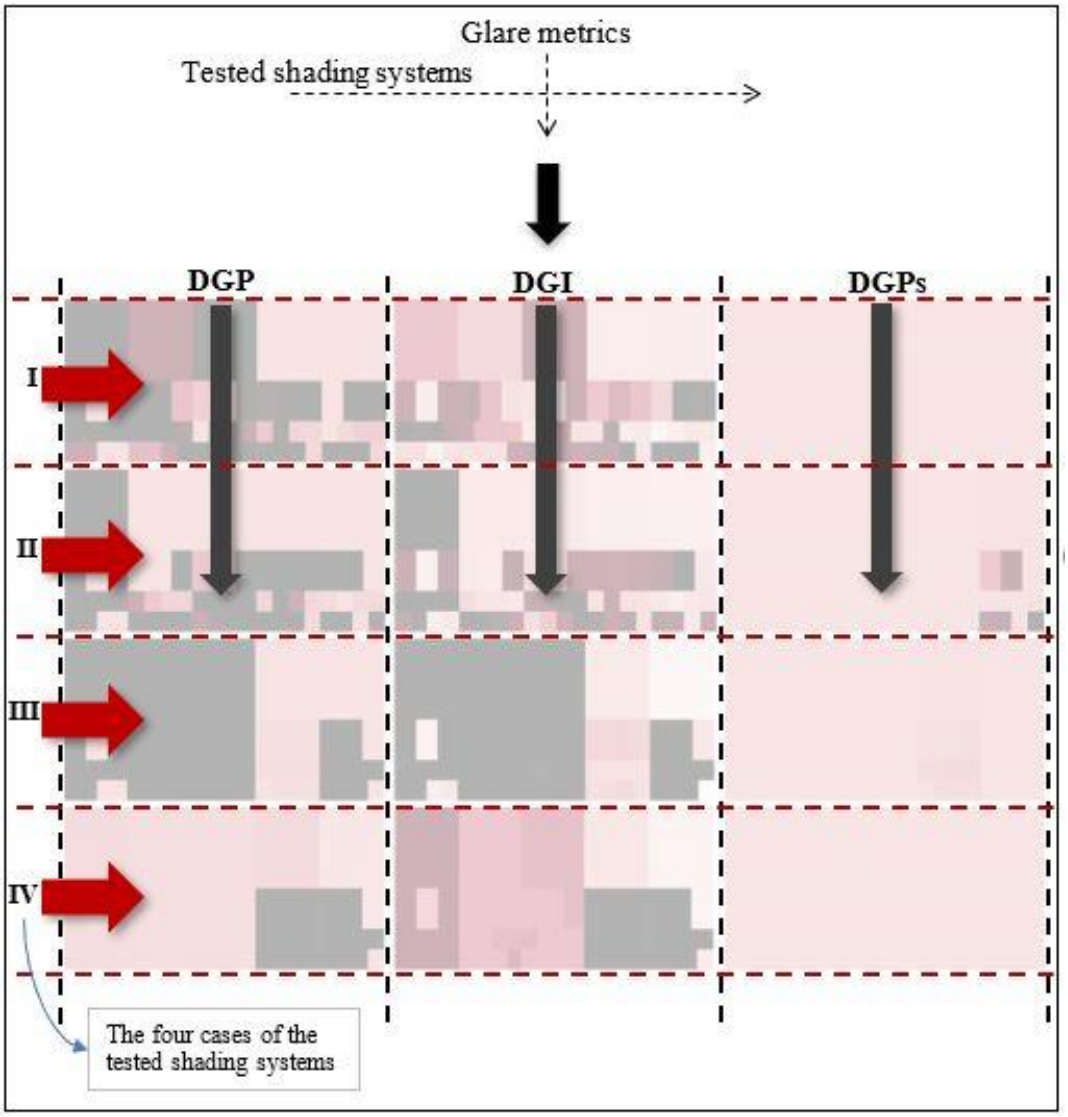

Figure 10b: Explanatory diagram of the space-time temporal map, used for the TPG illustration.

According to the previous explanatory diagrams, Figure 11 presented the results of the TPG per hour, tested metric and shading system for every observer's position.

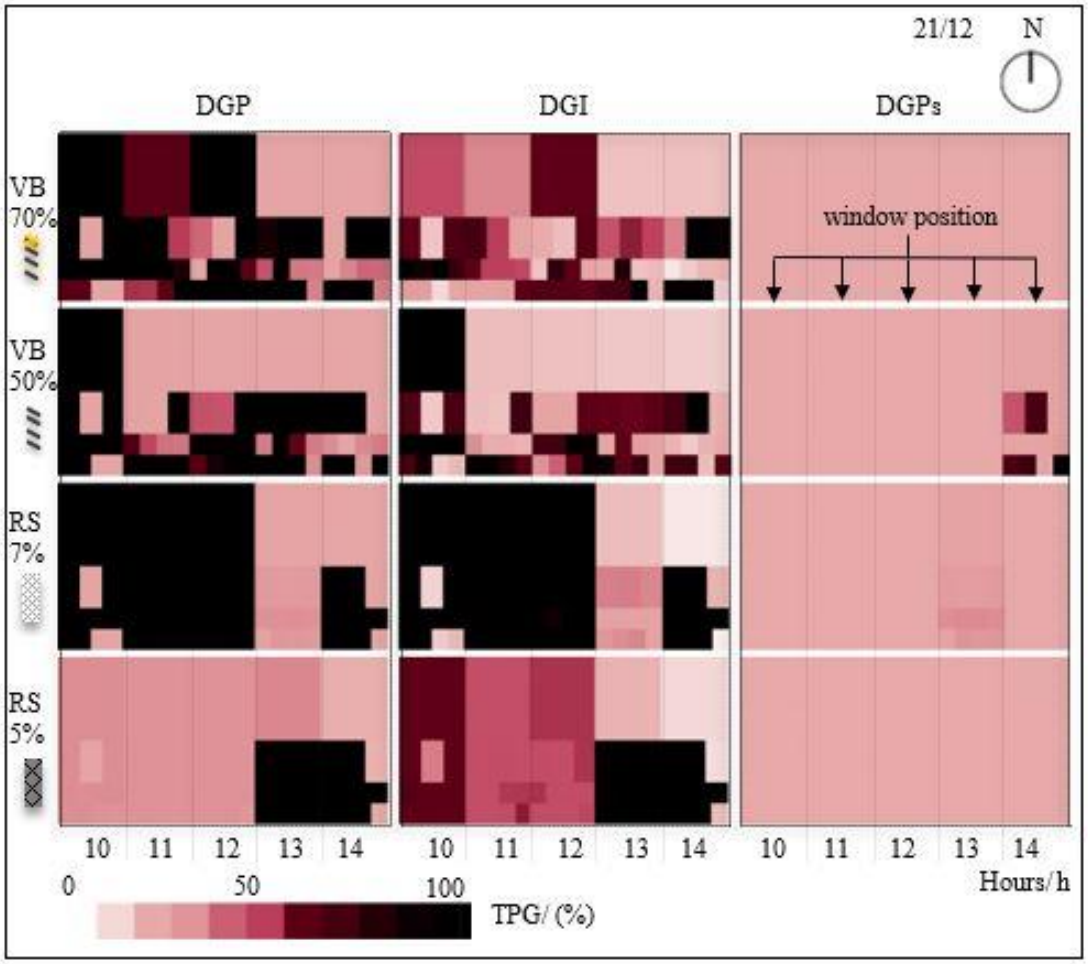

Figure 11: TPG map, consisted of the base case plan form[15], presenting the changed TPG per tested observer's position and the effect of the shading systems on glare control.

The DGP metric generally reported a higher risk for glare when compared to DGI and DGPs (Figure 11). The shading system of roller shades with 5% Openness Factor (OF) seemed to perform better that the rest, having glare risk mainly towards the sunset and in the 50% of the space close to window. The DGP and DGI results, though, indicated a similar pattern.

Figure 12 and 13 presented the space-time temporal maps for the rest tested days of 5/3 and 21/6 respectively.

[15] The plan, being presented here as a diagram for illustration purposes, is elongated towards South-North so that the results would be visible (see Figure 10a-b). The tested plan was not used as a scale for the pattern.

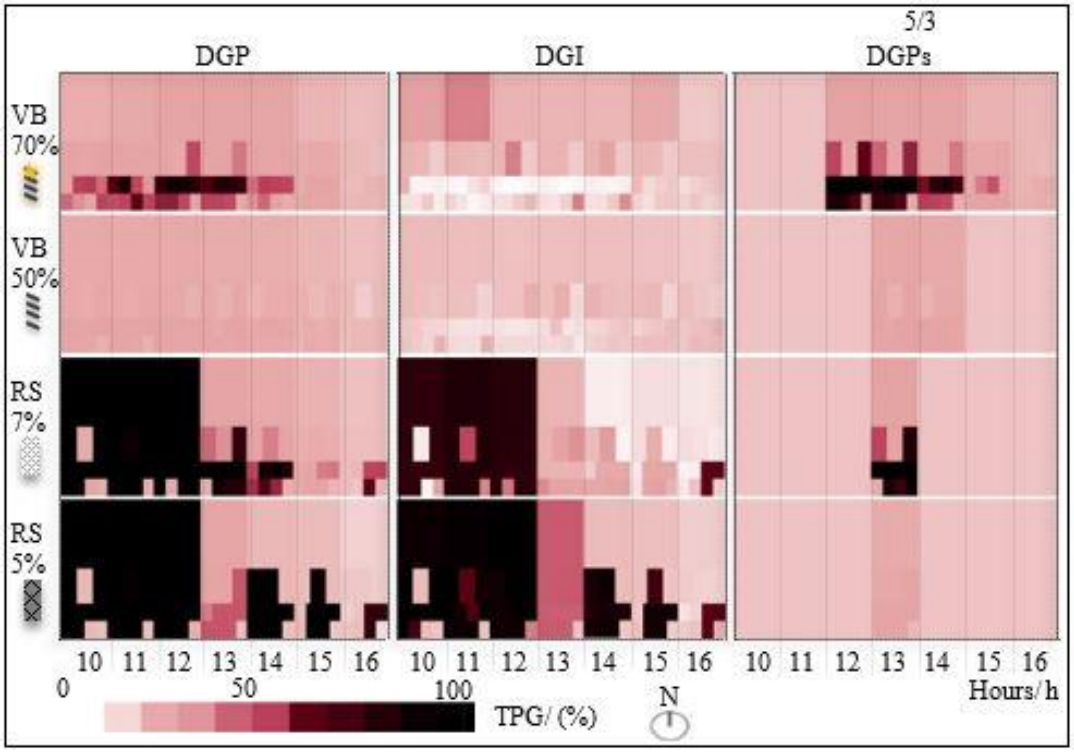

Figure 12: TPG map presenting the changed TPG during the 5th of March.

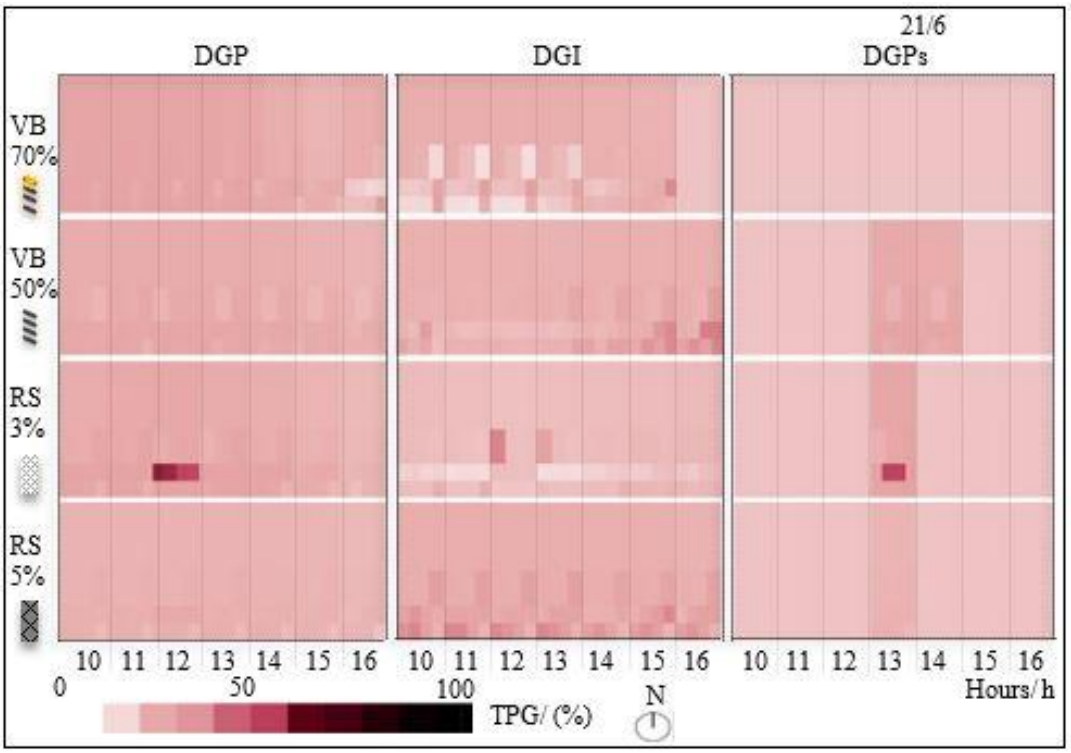

Figure 13: TPG map presenting the changed TPG during the 21st of June.

3.1.2 STG

For an analysis that would involve, also, the time parameter, the STG was investigated. Figure 14 presents the STG range of fluctuation for all the tested shading systems during 21/12 and 5/3. The performance of the studied shading systems regarding space-time glare was aiming for the STG to be below 50% (DGP-DGPs) and 40% (DGI).

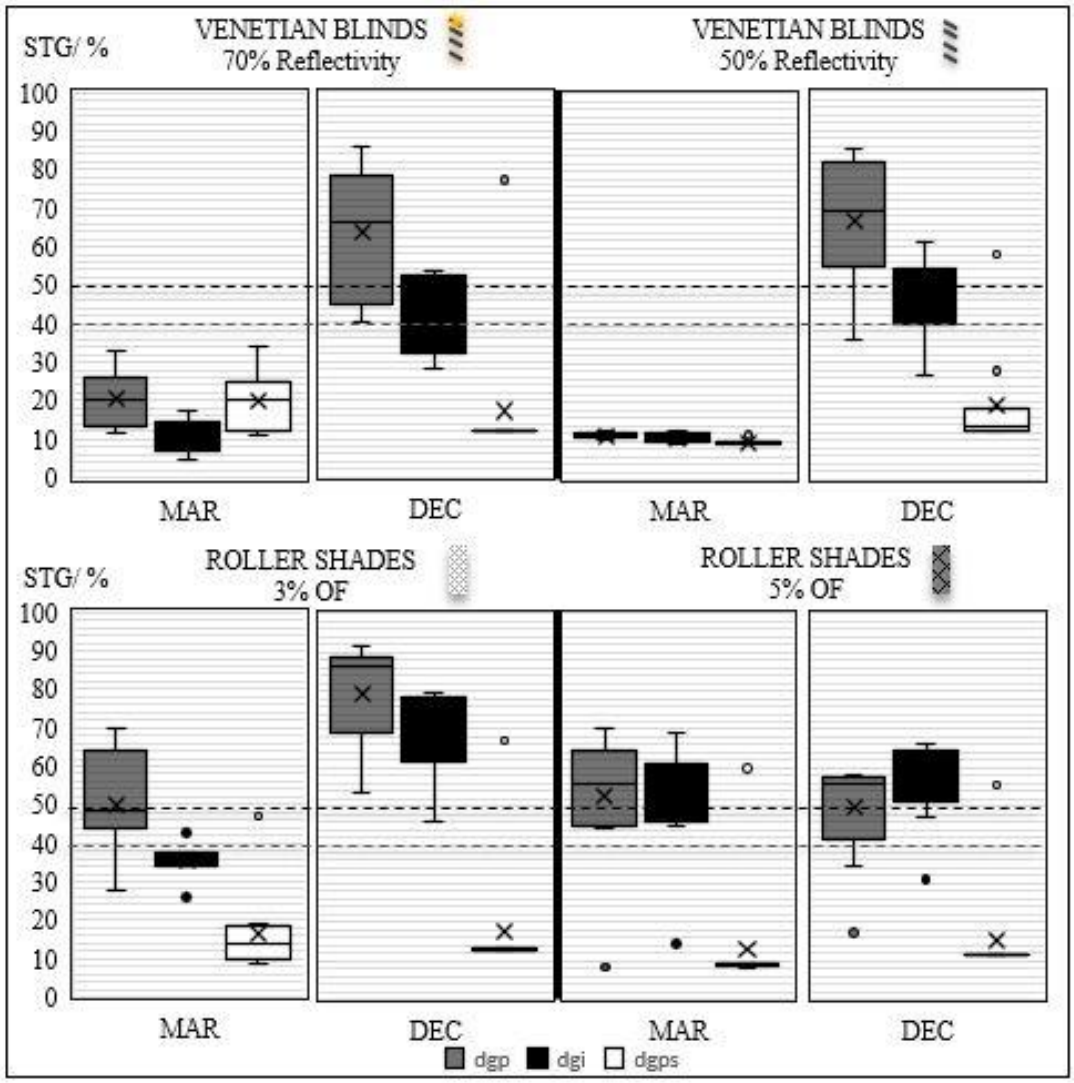

Figure 14: Graph presenting the STG during the investigated period for the four different fenestration systems.

This time the venetian blinds of 50% reflectance and the roller shades with 5% openness factor presented a rather good performance. The distribution of the STG in the space was investigated for those two advantageous systems. Figure 15 presents the distribution of the STG in the area of the case study during the critical 21/12 when the different shading systems were implemented.

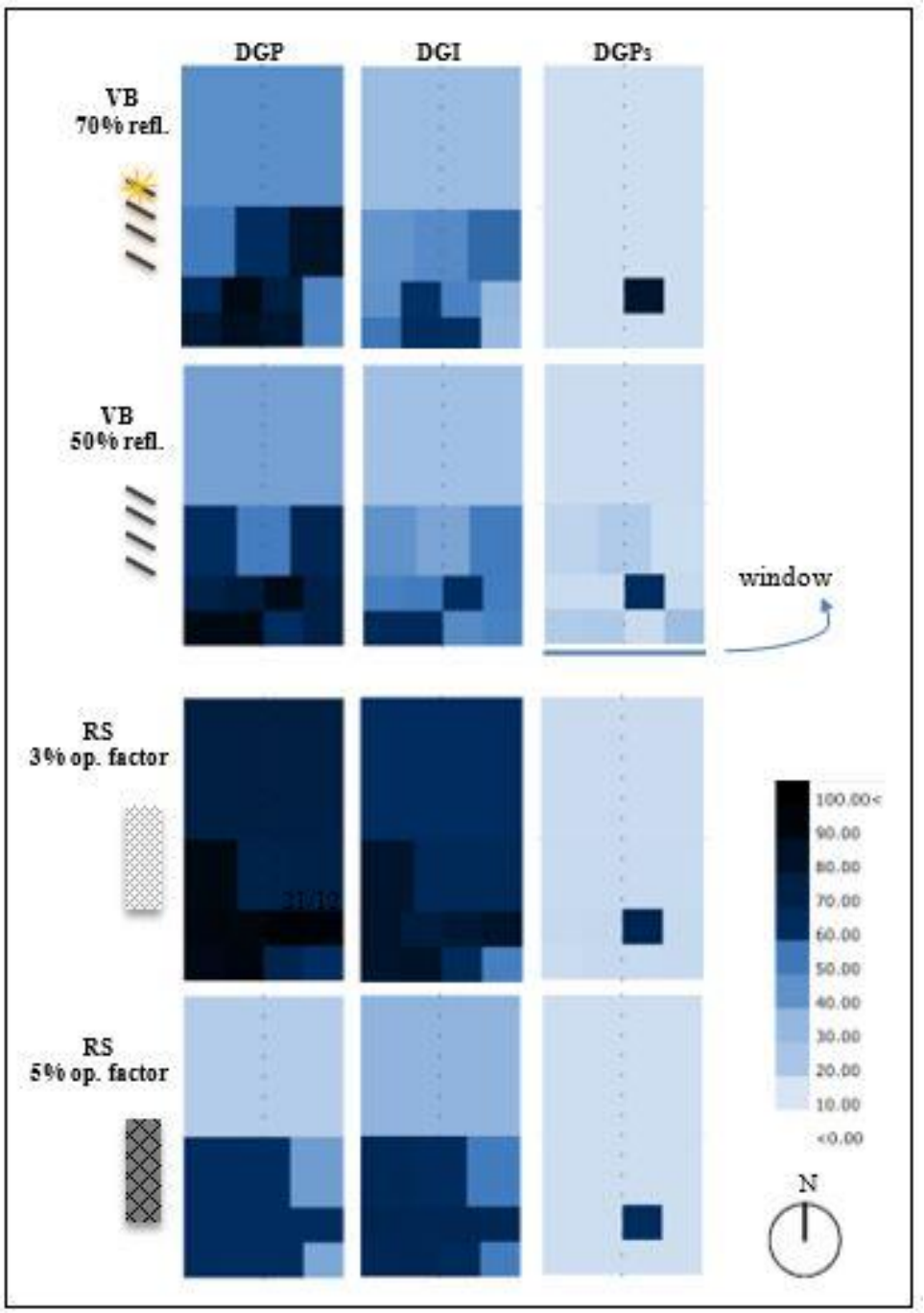

Figure 15: STG distribution in the tested area during the 21st of December[16].

[16] In Figure 15 the values of the DGPs were not presented as DGPs underestimated the risk for glare when compared to DGP and DGI during the TPG analysis.

It was found that, in both cases the glare risk could be expanded in the 50% of the area, though, the roller shades had a slightly decreased glare possibility. Figure 16 presents the STG distribution of the roller shades with 5% OF during the 21/12 and 5/3.

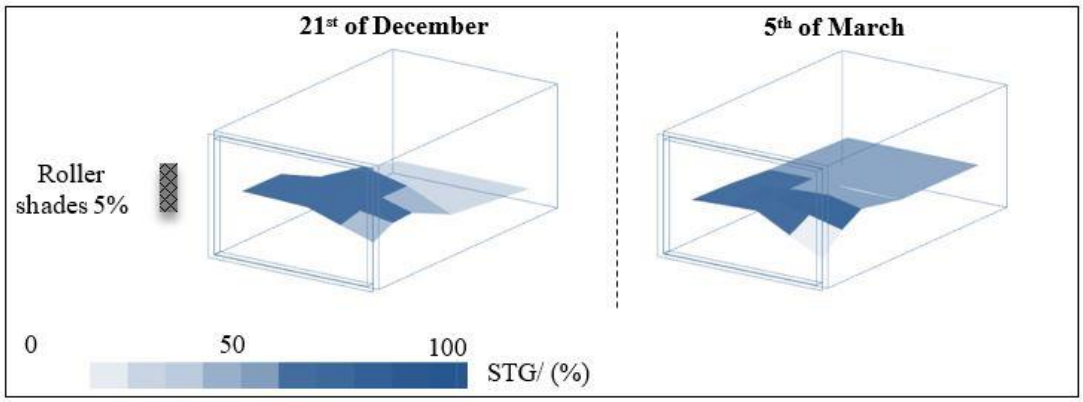

Figure 16: STG detail showing the glare distribution in space during the 21/12 and 5/3 (DGP values).

The two aforementioned shading systems, that showed the lowest values of glare risk, were compared in terms of illuminance levels and the possible area availability without glare problems (Figure 17a). Based on the analysis, the roller shades provided illuminance levels below the limit of 300lx in the whole space. The venetian blinds, on the other hand, resulted in low illuminance levels only in 43% of the space. By searching in more detail the space availability, it was found that the roller shades had a sharp change in the possible glare safe area during the studied time, in contrast to the venetian blinds, as shown in Figure 17b, fluctuating between 100% and 30%.

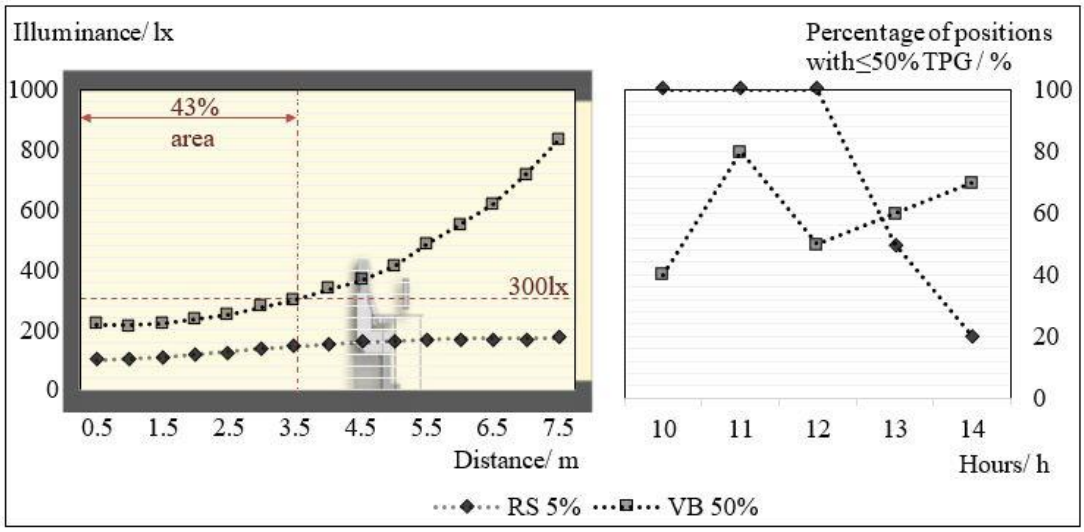

Figure 17a: Section of the studied geometry presenting the average illuminance levels during the 21/12 with different shading systems. Figure 17b: Graph showing the average area (according to DGP-DGI) where TPG ≤ 50% (or 40% for DGI), with different shading systems during 21/12.

4 Discussion

4.1 The conceptual framework

4.1.1 Adaptation possibility

G_{dir} was multiplied according to the proximity to the window, in order to introduce to the weighting system, the parameter of the increased glare risk severity when approaching closer the non-uniform glare source. However, this space weighting system derived after hypothesis during the current thesis. A possible empirical study upon this dependence will certainly reveal another weighting system, which is considered important for the future research in this field.

A recent study, presented by Bian and Ma (2018), indicated the possibility for a more specific time-based glare analysis that could influence the time parameter of the tested weighting system. According to this research, there is, in fact, an interrelation between the glare tolerance and the time duration. Since, the time step of their analysis was less than an hour, their rating was not implemented in the weighting system of this thesis. However, in the future, such detailed but also long-term time acceptability of glare conditions could contribute significantly to the glare evaluation.

It was a fact that testing multiple observer positions and gaze directions demanded an increased computational time. The rendering of all those necessary pictures was more time-consuming compared to the calculations regarding the adaptation possibility. However, even though Accelerad was not, eventually, preferred over Radiance, could be suggested for future implementation on the method for a further reduction of the computational time.

4.1.2 TPG and STG

Independently from the weighting system, the TPG concept introduces areas at lower risk for glare and, thus, more suitable for furniture positioning. For the exemplary cases in this thesis, for instance, approximately 50% of the space was indicated as having less variations in space availability under all the shading systems, during the 21st of December. This 50% was located 4m away from the window. Based on the TPG method and the resulted space distribution of glare per hour, the critical area for the performing of a demanding task would be approximately until 1.5m away from the window. During sunrise, DGP indicated low glare risk in 100% of the space under roller shades with 5% OF, while almost 100% problematic area under the venetian blinds.

Focusing only on the space availability provided by the roller shades throughout the day, it was notable that the glare free space reached 100% during a small period of time. However, the values fluctuated a lot between extremes. Such rapid variations in the percentage of the glare free area could have a negative impact on visual comfort. On the contrary, the venetian blinds seemed to have a more stable performance. In details, even though the values in this case did not reach 100% glare free area, they seemed to have a marginal fluctuation.

Since the trend in all cases changed per hour, the evaluation of the shading devices could not be carried out without the STG methodology. The fact that, the venetian blinds of 50%

reflectivity and the roller shades of 5% openness factor presented the best performance, could be interpreted as the effect of intermediate material properties. In case of roller shades, a very low openness factor, such as 3%, highlighted their ability to provide a homogenous dimming of light in space. The corresponding characteristic of the venetian blinds was the ability to regulate the light re-direction (70% reflectivity). In both shading systems, the implementation of materials with properties that moderate extreme behaviours, such as the use of increased OF[17] or decreased Reflectivity that actually reduces the patches, seemed to perform better.

The proposed method of TPG and STG could function as the base methodology to a future zonal glare analysis. Specifically, TPG already comprehended a weighting system based on the horizontal gaze direction and adaptation possibility in time. However, a proper evidence-based weighting system could be applied to this methodology.

4.2 Case study application

4.2.1 Glare metrics

Regarding the investigated glare metrics, it was interesting that, DGI and DGP-DGPs presented a reverse behaviour regarding the glare estimation when approaching the sunset without any shading system. Even though, only the correlation of space and lighting (contrast) provided a reasonable glare estimation, in a more elaborate index, taking all parameters into account (DGP), it was visible that the results differed. Additionally, DGP was adaptive to the shading system and the glare source, while DGI evaluated more generally the space. In case of the DGPs, by considering only the glare sources, the lighting conditions could not be evaluated in details and the results exhibited large differences with those of DGP and DGI.

Different metrics could indeed lead to different interpretation of the results, indicating the importance to implement specific metrics under the corresponding circumstances. A possible list, providing the correlation between the space circumstances and the indicators, or even the emerging of a specific criterion for the selection of the proper index, could be important.

4.2.2 Shading systems

Different shading systems could provide different amount of choices for the glare assessment. For this thesis a static shading system was examined, based upon preliminary analysis. The selection of the geometry and properties of the shading materials highly affected the light qualities in space. For instance, the venetian blinds could partially shade the glare source and, also, regulate the contrast, while the roller shades limited the possibilities of adaptation at each case.

[17] In the framework of glare protection.

5 Conclusion

This thesis proposed a conceptual framework to evaluate glare in a zonal and dynamic way by using existing glare indexes. The conceptual framework was applied on a case study. The proposed methodology in this thesis currently relies on arbitrary weighting systems and assumptions taking into consideration the adaptation possibility due head movement and time aspect.

The conceptual framework may potentially simplify the early design of space. The method should allow to place the furniture/partition at an early design stage by handing in to the architect a simple chart as, for example, in Figure 15. However, the thesis shows that the conceptual framework is expensive in terms of computational time, even for glare analysis with hourly step. The main issue is that a high number of image-based simulations need to be run. This issue may be solved in the future, when supercomputers will be available to the general public and lighting simulation may rely on more efficient engines, like the aforementioned Accelerad.

In the meanwhile, efforts can be directed in proposing an evidence-based weighting system for the directional and temporal acceptability of glare, which is the most critical part of this work.

Summary

A method towards a dynamic daylight glare evaluation in the early stage of design was developed in this thesis, using existing glare metrics under multiple observer positions and gazes. The results pointed out that it is possible for a zonal characterization regarding glare sensation to be achieved with the combination of multiple existing metrics and a weighting system, named the *adaptation possibility*.

Initially, a literature review was conducted in order to specify the limitations of the existing glare metrics and the different practices used for glare evaluation. Then the thesis continued in the definition of the proposed methodology and the case study on which the method would be tested.

The proposed methodology for a dynamic and zonal glare evaluation would account for different gaze directions and observer positions, as well as, the adaptation possibility in terms of head rotation and glare duration. Multiple glare metrics were used in the method as the literature review indicated that, there is a need either for an enhanced glare metric that would meet the current limitations or for a combination of the existing ones. Thus, the existing glare metrics of DGP, DGPs and DGI were implemented in the method. For the extraction of one glare value per position, two indicators were created named the *Total Point Glare* (TPG) and the *Space-Time Glare* (STG) based on a point-in-time analysis and a period of time respectively. It is important to note that, the method included arbitrary assumptions which needed to be validated 'in situ'.

The case study was that of a hypothetical library room in Stockholm with one fully glazed façade facing South. Additionally, the performance of different shading systems, such as venetian blinds and roller shades, were tested. After a direct sun analysis at eye level, a specific grid was formed indicating the different possible positions of the observer in the space. The observer would be able to rotate his head in each position and, thus, the study would account for multiple gazes with a fixed visual centre directed towards a computer screen. The time step of the analysis was that of 1 hour.

The results of the study indicate that provided glare free area under roller shades reached 100% during a small period of time. However, the glare free area coverage fluctuated a lot between extremes (from 100% to only 20% of the total space). Such rapid variations could potentially have a negative impact on visual comfort counteracting any temporary glare protection. On the contrary, the performance of the venetian blinds seemed to be more stable, even though the glare free area coverage did not reach 100% of the space.

It was found that, even though the method allows the placement of the furniture/partition at an early design stage, it is still quite expensive in terms of computational time. This issue could be solved in the future when supercomputers will be available to the general public and lighting simulation may rely on more efficient engines.

Since the method derived from researched rules of thumb and reasoneable hypothesis implemented in a virtual model, should be further investigated and validated with empirical studies with human subjects.

Regarding the case study, it was found that, different metrics could evaluate the space differently according to the parameter that they are based on (e.g. Contrast, beam illuminance, dim space conditions), indicating the importance to implement specific metrics under the corresponding circumstances. Different shading systems could provide different choices for the glare assessment. The examined statistic shading systems indicated that the venetian blinds could partially shade the glare source and regulate the contrast, while the roller shades limited the possibilities of adaptation at each case. It was interesting to observe that the DGP indicated low glare risk in 100% of the space under roller shades, while almost 100% problematic area under the venetian blinds.

Popular Science Summary

A concept to evaluate dynamic daylight glare

Glare is a physiological phenomenon influencing visual comfort. While disability glare is easier to assess, discomfort glare has been rather difficult to be estimated. Most of the metrics found in literature are, to some extent, reliable predictors of glare. However, they refer to specific conditions for *a point in time* and *a point in space with a certain direction of gaze*. This implies that they are mostly useful during an advanced design stage. But how reliable would be a daylight glare evaluation of a whole space, based only on one view and a point-in-time analysis? More and more daylight researchers conclude that current glare estimation practices form a base for development. This thesis proposes a specific methodology for a dynamic and zonal glare evaluation during a period of time. The aim is not the development of a new glare metric, but rather the combination of the existing ones in an earlier design stage.

The proposed methodology considers different observer positions and gaze directions, while accounting for the adaptation possibility in terms of head rotation and glare duration. Three glare metrics were implemented, the DGP, DGI and DGPs, as they could enhance the total glare evaluation by describing the glare sensation either based on contrast and/or direct sunlight penetration. Eventually, two indicators were developed, the *Total Point Glare* (TPG), that outputs one glare indication value per position and point-in-time, and the *Space-Time Glare* (STG), that provided one glare prediction value per position during a longer period of time.

For the development of the aforementioned method, a virtual model of a hypothetical library room in Stockholm was used, having a fully glazed façade towards South. The performed analysis was grid-based, in order to simulate the possible movement of the occupant in the space. Additionally, the occupant could rotate his head so, that multiple gazes would be examined. The study considered the impact of two shading systems, namely venetian blinds and roller shades, on glare risk assessments.

Zonal glare analysis could drastically improve the design of space by evaluating different areas in terms of glare probability and glare free space availability. Even though the method allows the placement of the furniture/partition at an early design stage, it is quite expensive in terms of computational time. This issue could be solved in the future when supercomputers will be available to the general public and lighting simulation may rely on more efficient engines. Since the method derived from reasoned assumptions and hypothesis, should be further investigated and validated with empirical data.

The investigated glare indices presented a similar pattern regarding the critical zones of space. Different metrics could lead to different interpretation of the results, indicating the importance to implement specific metrics under the corresponding circumstances. Furthermore, regarding the tested shading systems, it was shown that the diffusive systems could maintain approximately the same illuminance levels. However, the provided glare safe area coverage would vary a lot during the day, counteracting the seemingly enhanced visual comfort.

References

Altomonte, S. *et al.* (2016) 'Visual task difficulty and temporal influences in glare response', *Building and Environment*. 95, pp. 209–226.

Andersen, M. (2015) 'Unweaving the human response in daylighting design', *Building and Environment*, 91, pp. 101–117.

Atzeri, A. M. *et al.* (2016) 'Comfort metrics for an integrated evaluation of buildings performance', *Energy and Buildings*. 127, pp. 411–424.

Bargary, G. *et al.* (2015) 'Cortical hyperexcitability and sensitivity to discomfort glare', *Neuropsychologia*. 69, pp. 194–200.

Bellia, L. *et al.* (2008) 'Daylight glare: A review of discomfort indexes', in *Visual quality and energy efficiency in indoor lighting: today for tomorrow*. Rome, Italy.

Bian, Y. and Ma, Y. (2018) 'Subjective survey & simulation analysis of time-based visual comfort in daylit spaces', *Building and Environment*. 131, pp. 63–73.

Boyce, P. R. (2003) *Human factors in lighting*. 2. ed. London [u.a.]: Taylor & Francis.

BREEAM (2017) 'BREEAM-SE New Construction', *Technical Manual*. s.l.: SGBC and BRE Global, 1.0, pp. 76–90.

Carlucci, S. *et al.* (2015) 'A review of indices for assessing visual comfort with a view to their use in optimization processes to support building integrated design', *Renewable and Sustainable Energy Reviews*. 47, pp. 1016–1033.

Chan, Y.-C., Tzempelikos, A. and Konstantzos, I. (2015) 'A systematic method for selecting roller shade properties for glare protection', *Energy and Buildings*. 92, pp. 81–94.

CIE (1995) *Discomfort glare in the interior working environment*. Vienna (Austria).

CIE (2002) *Glare from Small, Large and Complex Sources*. Vienna (Austria).

Core Studio (2018) *TT Toolbox, Robert McNeel and Associates*. Available at: http://www.food4rhino.com/app/tt-toolbox (Accessed: 3 April 2018).

Dubois, M.-C. (2001) *Impact of Shading Devices on Daylight Quality in Offices: Simulations with Radiance*. Lund University, Division of Energy and Building Design.

Eble-Hankins, M. L. and Waters, C. E. (2009) 'Subjective Impression of Discomfort Glare from Sources of Non-Uniform Luminance', *LEUKOS*. Taylor & Francis, 6(1), pp. 51–77.

Einhorn, H. D. (1969) 'A new method for the assessment of discomfort glare', *Lighting Research & Technology*. SAGE Publications, 1(4), pp. 235–247.

Einhorn, H. D. (1979) 'Discomfort glare: a formula to bridge differences', *Lighting*

Research and Technology. SAGE Publications, 11(2), pp. 90–94.

Fritz, R. and Mcneil, A. (2018) *Radiance, Lawrence Berkeley National Laboratory (LBNL)*. Available at: https://www.radiance-online.org/about (Accessed: 3 April 2018).

'Grasshopper 3D' (2018). Robert McNeel and Associates. Available at: http://www.grasshopper3d.com/.

Hirning, M. B. (2014) *The application of luminance mapping to discomfort glare: a modified glare index for green buildings*. Queensland University of Technology.

Hirning, M. B., Isoardi, G. L. and Garcia-Hansen, V. R. (2017) 'Prediction of discomfort glare from windows under tropical skies', *Building and Environment*. 113, pp. 107–120.

Hopkinson, R. G. (1972) 'Glare from daylighting in buildings', *Applied Ergonomics*. 3(4), pp. 206–215.

IES (2012) *Approved Method: IES Spatial Daylight Autonomy (sDA) and Annual Sunlight Exposure (ASE)*.

Iwata, T. *et al.* (1990) 'Discomfort caused by wide-source glare', *Energy and Buildings*. Elsevier, 15(3–4), pp. 391–398.

Iwata, T. and Tokura, M. (1997) 'Position Index for a glare source located below the line of vision', *Lighting Research & Technology*. 29(3), pp. 172–178.

Iwata, T. and Tokura, M. (1998) 'Examination of the limitations of predicted glare sensation vote (PGSV) as a glare index for a large source: Towards a comprehensive development of discomfort glare evaluation', *Lighting Research & Technology*. 30(2), pp. 81–88.

Jakubiec, A. (2014) *The Use of Visual Comfort Metrics in the Design of Daylit Spaces*. Massachusetts Institute of Technology.

Jakubiec, J. A. and Reinhart, C. F. (2011) 'DIVA 2.0: Integrating daylight and thermal simulations using rhinoceros 3D, DAYSIM and EnergyPlus', in *Proceedings of Building Simulation 2011: 12th Conference of International Building Performance Simulation Association;* pp. 2202–2209.

Jakubiec, J. A. and Reinhart, C. F. (2012) 'The 'adaptive zone'-A concept for assessing discomfort glare throughout daylit spaces', *Lighting Research and Technology*. 44(2), pp. 149–170.

Jakubiec, J. A. and Reinhart, C. F. (2016) 'A Concept for Predicting Occupants' Long-Term Visual Comfort within Daylit Spaces', *LEUKOS - Journal of Illuminating Engineering Society of North America*. 12(4), pp. 185–202.

Jones, N. L. (2017a) *Accelerad, Lawrence Berkeley National Laboratory (LBNL)*. Available at: https://nljones.github.io/Accelerad/index.html (Accessed: 3 April 2018).

Jones, N. L. (2017b) *Validated Interactive Daylighting Analysis for Architectural Design*. Massachusetts Institute of Technology.

Kim, W., Han, H. and Kim, J. T. (2009) 'The position index of a glare source at the borderline between comfort and discomfort (BCD) in the whole visual field', *Building and Environment*. 44(5), pp. 1017–1023.

Konstantzos, I. *et al.* (2015) 'View clarity index: A new metric to evaluate clarity of view through window shades', *Building and Environment*, 90, pp. 206–214.

Konstantzos, I. and Tzempelikos, A. (2017) 'Daylight glare evaluation with the sun in the field of view through window shades', *Building and Environment*. 113, pp. 65–77.

Konstantzos, I., Tzempelikos, A. and Chan, Y.-C. (2015) 'Experimental and simulation analysis of daylight glare probability inoffices with dynamic window shades', *Building and Environment*. 87, pp. 244–254.

LEED (2018) 'Building Design and Construction Agenda'. s.l.: USGBC, 4, pp. 132–134.

Lim, G.-H. *et al.* (2017) 'Daylight performance and users' visual appraisal for green building offices in Malaysia', *Energy and Buildings*, 141, pp. 175–185. doi: //doi.org/10.1016/j.enbuild.2017.02.028.

Luckiesh, M. and Guth, S. K. (1949) 'Brightnesses in visual field at borderline between comfort and discomfort', *Illuminating engineering*, 44(11), pp. 650–670.

McNeil, A. (2016) *BSDFviewer, Lawrence Berkeley National Laboratory (LBNL)*. Available at: https://www.radiance-online.org/download-install/third-party-utilities/bsdf-viewer (Accessed: 3 April 2018).

McNeil, A. (2017) *Evalglare, Lawrence Berkeley National Laboratory (LBNL)*. Available at: https://www.radiance-online.org/learning/documentation/manual-pages/pdfs/evalglare.pdf/view (Accessed: 3 April 2018).

McNeil, A. and Burrell, G. (2016) 'Applicability of DGP and DGI for evaluating glare in a brightly daylit space', *Proceedings of SimBuild*, 6(1).

Mitchell, R. *et al.* (2013) *THERM 6.3 / WINDOW 6.3 NFRC Simulation Manual*. Lawrence Berkeley National Laboratory (LBNL). Available at: https://windows.lbl.gov/software/window.

Petherbridge, P. and Hopkinson, R. G. (1950) 'Discomfort glare and the lighting of buildings', *Lighting Research and Technology*, 15, 2(2 IEStrans), pp. 39–79.

Piacentino, G. (2013) *GHPython, Robert McNeel and Associates*. Available at: http://www.food4rhino.com/app/ghpython (Accessed: 3 April 2018).

Piccolo, A. and Simone, F. (2009) 'Effect of switchable glazing on discomfort glare from windows', *Building and Environment*, 44(6), pp. 1171–1180.

prEN 17037 (2016) *Daylight of buildings, European Standard*. British Standards Institution (BSI).

Reinhart, C. F. and Wienold, J. (2011) 'The daylighting dashboard – A simulation-based design analysis for daylit spaces', *Building and Environment*, 46(2), pp. 386–396.

'Rhinoceros 3D' (2018). Robert McNeel and Associates. Available at: https://www.rhino3d.com/.

Robinson, W. *et al.* (1962) 'The Development of the IES Glare Index System: Contributed by the Luminance Study Panel of the IES Technical Committee', *Transactions of the Illuminating Engineering Society*. SAGE Publications, 27(1_IEStrans), pp. 9–26.

Sadeghipour Roudsari, M. and Pak, M. (2013) 'Ladybug: A parametric environmental plugin for Grasshopper to help designers create an environmentally-conscious design', in *13th Conference of International Building Performance Simulation Association*, pp. 3128–3135.

Suk, J. Y., Schiler, M. and Kensek, K. (2017) 'Investigation of existing discomfort glare indices using human subject study data', *Building and Environment*. 113, pp. 121–130.

Tokura, M., Iwata, T. and Shukuya, M. (1996) 'Experimental study on discomfort glare caused by windows part 3: Development of a method for evaluating discomfort glare from a large light source', *Journal of Architecture and Planning (Transactions of AIJ)*, 61(489), pp. 17–25.

Tuaycharoen, N. and Tregenza, P. R. (2007) 'View and discomfort glare from windows', *Lighting Research and Technology*, 39(2), pp. 185–198.

Tzempelikos, A. (2017) 'Advances on daylighting and visual comfort research', *Building and Environment*. 113, pp. 1–4.

Tzempelikos, A. and Chan, Y.-C. (2016) 'Estimating detailed optical properties of window shades from basic available data and modeling implications on daylighting and visual comfort', *Energy and Buildings*. 126, pp. 396–407.

Wienold, J. (2007) 'Dynamic simulation of blind control strategies for visual comfort and energy balance analysis', in *Building Simulation*. Beijing, China: IPBSA, pp. 1197–1204.

Wienold, J. (2009) 'Dynamic daylight glare evaluation', in *IBPSA 2009 - International Building Performance Simulation Association 2009; 11th International IBPSA Conference - Building Simulation 2009, BS 2009*. pp. 944–951.

Wienold, J. and Christoffersen, J. (2006) 'Evaluation methods and development of a new glare prediction model for daylight environments with the use of CCD cameras', *Energy and Buildings*. 38(7), pp. 743–757.

Van Den Wymelenberg, K., Inanici, M. and Johnson, P. (2010) 'The effect of luminance distribution patterns on occupant preference in a daylit office environment', *LEUKOS* -

Journal of Illuminating Engineering Society of North America. 7(2), pp. 103–122.

Yamin Garreton, J. A. *et al.* (2015) 'Degree of eye opening: A new discomfort glare indicator', *Building and Environment*. 88, pp. 142–150.

APPENDIX A

A.1 Glare Metrics

The entire formula of the VCP glare metric can be found below.

$$\boldsymbol{VCP = \frac{100}{\sqrt{2\pi}} \cdot \int_{-\infty}^{6.374-1.3227\, ln(DGR)} \left(e^{-t^2/2} \cdot dt \right)} \quad [-] \quad (22)$$

where,

$$\boldsymbol{VCP = \begin{cases} 279 - 110(log_{10}\, DGR)\,, for\ DGR = 55{\sim}200 \\ 279 - 110(log_{10}\, DGR) + 350(log_{10}(DGR) - 2.08)^5 \\ \qquad\qquad ,for\ \neq 55{\sim}200 \end{cases}}$$

and, $\boldsymbol{DGR = \left(\sum_{i=1}^{n} \frac{L(20.4\omega_s + 1.52\omega_s^{0.2} - 0.075)}{2PL_f^{0.44}} \right)^{\alpha}}$

The Guth Position Index (P) used in several glare equations indicating the observer, derived from the following formulas.

- Above the line of sight (Luckiesh and Guth, 1949):

$$\ln P = \left(35.2 - 0.31889\tau - 1.22e^{-2\tau/9}\right) 10^{-3}\sigma + (21 + 0.26667\tau - 0.002963\tau^2) 10^{-5}\sigma^2 \quad [-] \quad (23)$$

- Below the line of sight (Iwata and Tokura, 1997):

$$P = 1 + 0.8\frac{R}{D} \quad \text{, when } R < 0.6D \quad [-] \quad (24)$$

$$P = 1 + 1.2\frac{R}{D} \quad \text{, when } R \geq 0.6D \quad [-] \quad (25)$$

$$\text{where, } R = \sqrt{H^2 + Y^2} \quad [\text{m}] \quad (26)$$

Table 7: The following table presents the treshold for the examined glare metrics.

Macro-categories	***VCP***	***BRS/GI***	***CGI***	***DGI***	***UGR***	***PGSV***	***DGP /DGPs /eDGPs***	***DGPmod***
Imperceptible	80-100		≥10		≥10		<0.35	<0.35
Just perceptible		10	≥13	>16	≥13	0		
Noticeable				>18				
Perceptible	60-80	13	≥16		≥16		0.35–0.40	0.35–0.44
Just acceptable		16	≥19	>20	≥19	1		
Acceptable		19		>22				
Just comfortable						2		
Unacceptable			≥22		≥22			
Just uncomfortable		22	≥25	>24	≥25			
Uncomfortable		25	≥28	>26	≥28			
Disturbing	40-60						0.40–0.45	0.44–0.45
Just intolerable		28		28		3		
Intolerable	<40			>28			>0.45	>0.45

The glare metrics that were not eventually used were:

- VCP, BRS, CGI, UGR and UGP, as they would be more appropriate glare predictors under artificial lighting conditions and uniform glare sources.
- PGSV, as the parameter indicating the shape of the source, namely the modified solid angle (Ω_s) used by DGI, was not included in the formula (Iwata and Tokura, 1998). This occurred due to the fact that, the PGSV assumes, that the observer would gaze straight towards the window (Boyce, 2003).
- DGP_{mod} were not implemented in the method, as both criteria derived after experiments specifically with roller shades and could not be generalized for other glare control strategies.
- eDGPs , as the reduced simulation time of the eDGPs arose from the fact that, the precise ray bounces inside the tested geometry were not taken into account (-ab 0) (Wienold, 2009). Such limitation could be critical when glare control systems, such as venetian blinds, were to be investigated, leading to inaccurate results.

A.2 Input Parameters

Table 8: The inserted Rad Parameters.

-ab	6	**-ds**	0.15
-ad	2048	**-dt**	0.05
-as	1024	**-dc**	0.75
-ar	512	**-dr**	3
-aa	0.1	**-dp**	512
-ps	2	**-st**	0.15
-pt	0.05	**-lr**	8
-pj	0.9	**-lw**	0.005
-dj	0.7		

APPENDIX B

B.1 Base case analysis

The base case analysis helped in finding the periods at higher glare risk, for which the proposed method was applied. This operation supports a reduction of the number of simulations to be performed and reduces the computational time. Figure 18 presents the percentage of the studied space with direct sunlight per hour throughout a year for two orientations, South and West. The 5th of March, as well as, the 21st of June and the possible worst case scenario of the 21st of December were studied, in agreement with Dubois (2001). The South orientation was chosen as it received in total more hours of direct sunlight compared to the West. No glare risk was found under overcast sky conditions (Figure 19). The risk for glare was also reduced under clear sky with sun during 17:00-19:00 (21/6) and 17:00 (5/3) (Figure 20). Thus, those cases were excluded from the study.

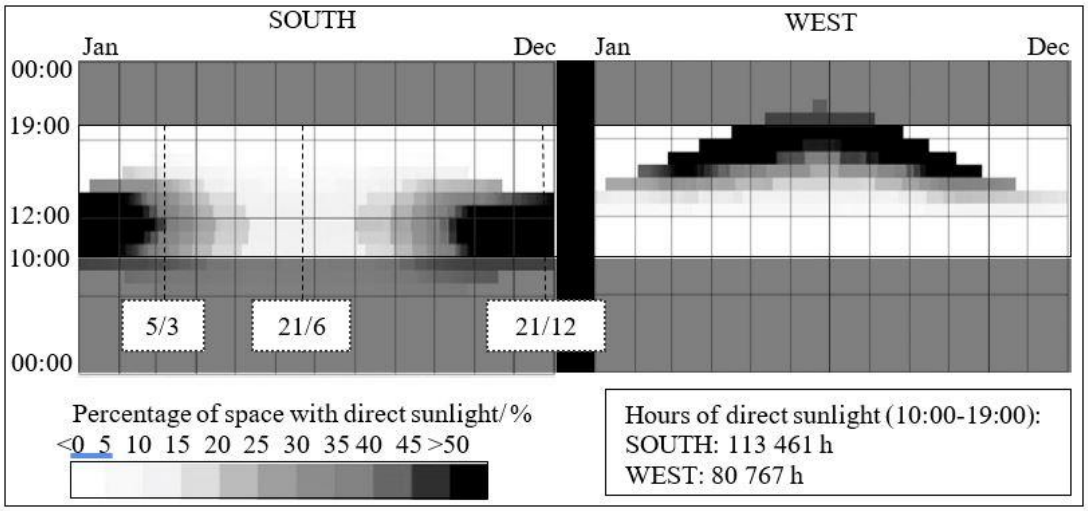

Figure 18: Diagram presenting the percent of floor in direct sun (%) per hour throughout the year.

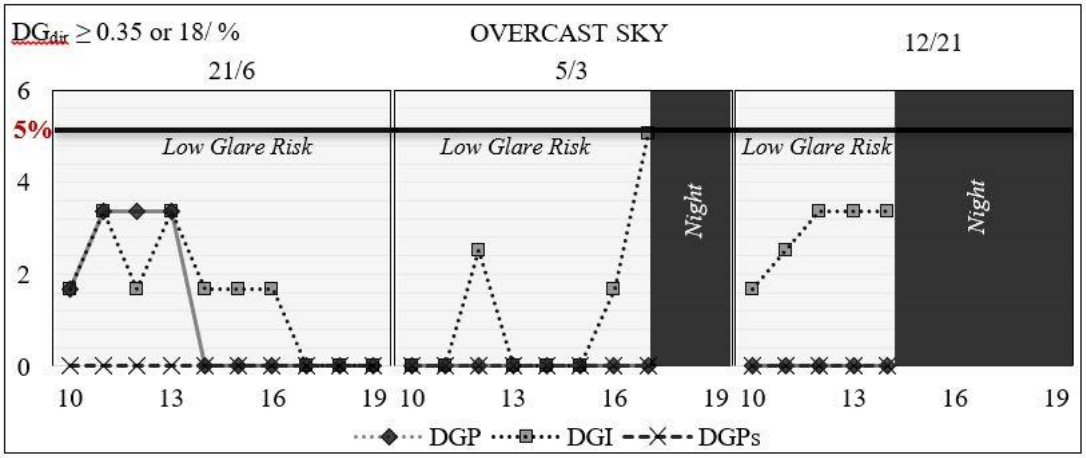

Figure 19: The percentage of all the directional glare predictions with increased glare risk (≥0.35, 18) per tested hour under overcast sky.

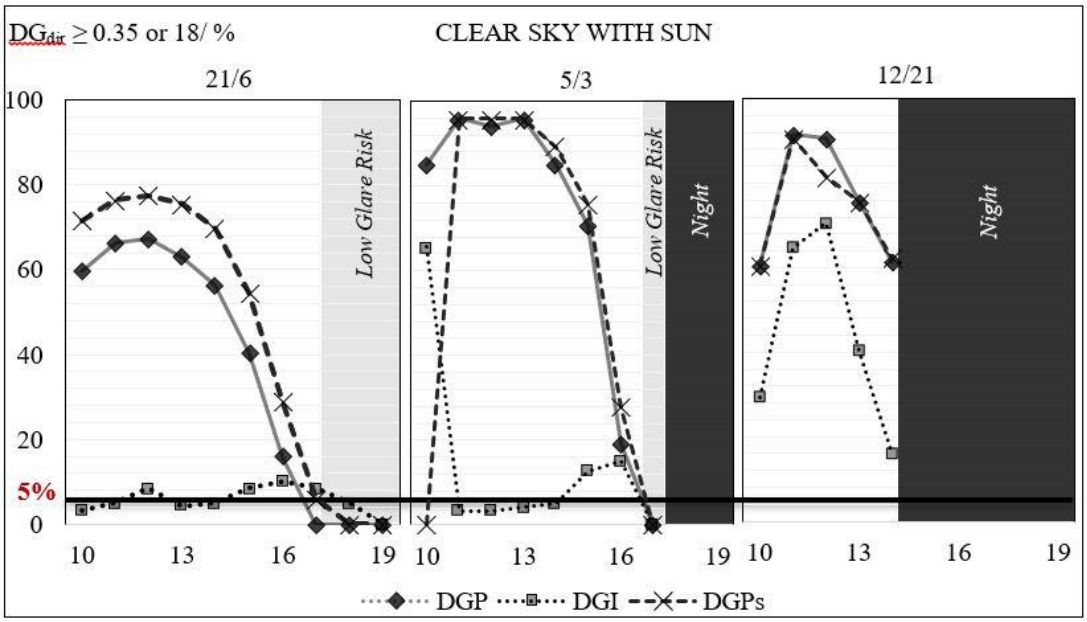

Figure 20: Graphs presenting the percentage of all the directional glare predictions with increased glare risk (≥0.35) per tested hour.

Figure 21 presents the glare risk prediction per hour for two critical observer positions during the 12/21. The first tested point was in front of the window and the second 5m from the window. The tested gaze was directed towards the window.

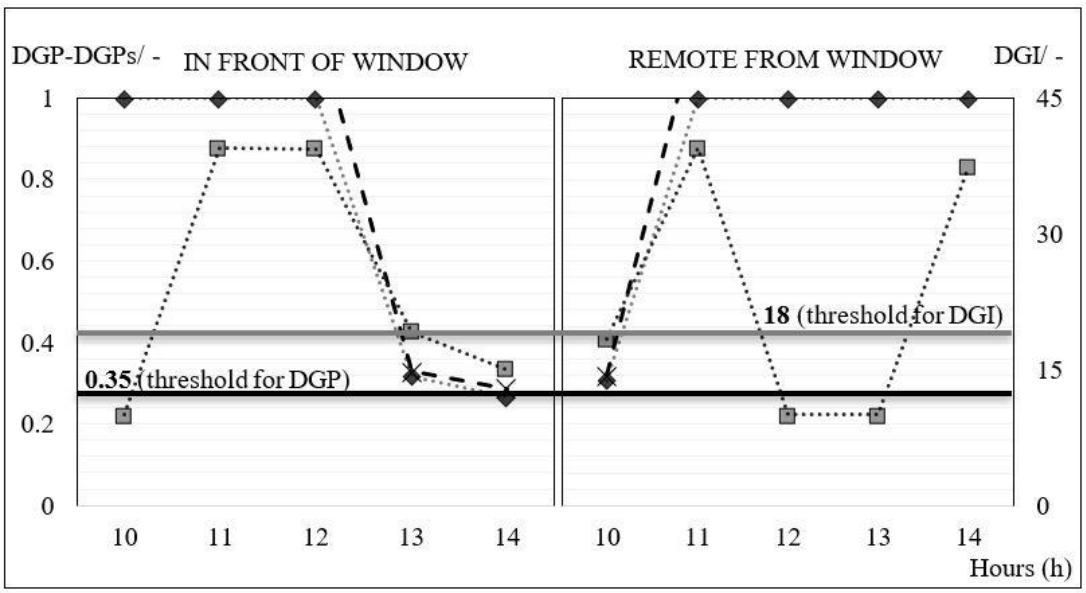

Figure 21: Graphs indicating the difference between the glare metrics in the 2 tested positions.

B.2 Shading Systems

A parametric study was conducted for the selection of the appropriate fixed slat angle and operational length for the venetian blinds. The scope was not an optimization of the used shading system but the selection of such geometry that would seemingly result in less glare risk when accounting only the illuminances as a criterion. Figure 22 presents the effect on the illuminance levels, due to the changed slat angle during 21/6, when different lengths were implemented. The chosen geometry, illustrated in Figure 23, presented low percentages above 3000lx and below 300lx.

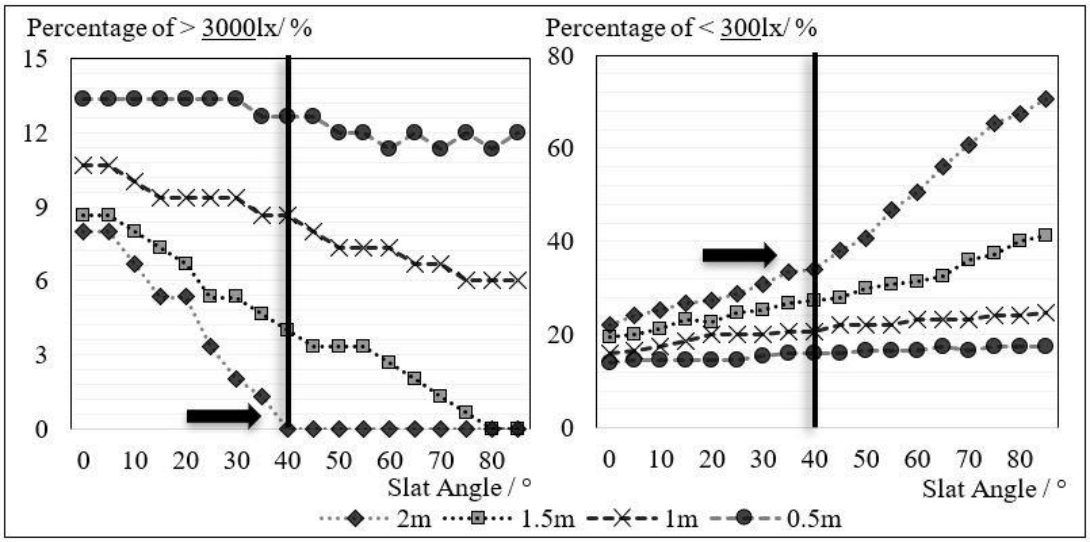

Figure 22: Percentage of the Illuminance levels on the tested section and the effect of the changed length and slat angle of the venetian blinds.

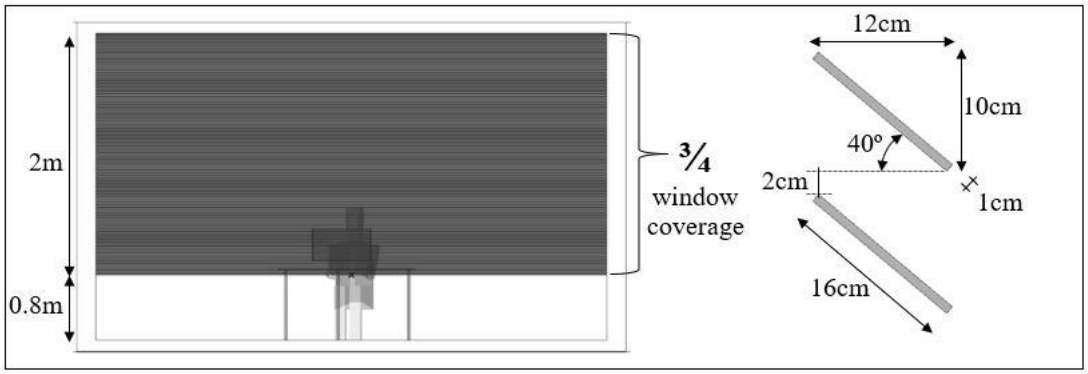

Figure 23: The chosen geometry of the venetian blinds in operation.

The possible performance regarding glare risk of the 2m length venetian blinds was tested. For this, the specular reflectances falling on different areas of the space were examined during the 21/12 with the slat angles being changed (Figure 24). The 40° outperformed in this case, as well, presenting a combination of decreased levels on the critical visual field and an increased number of direct rays gathered towards the ceiling.

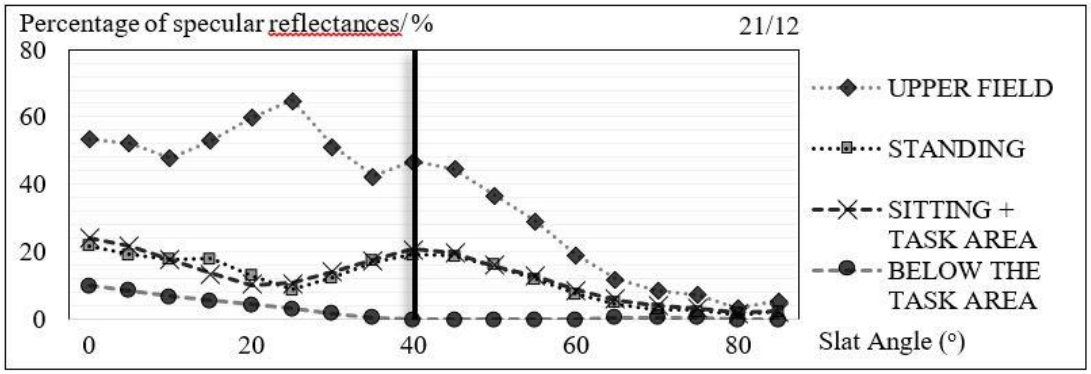

Figure 24: Percentage of specular reflectances (2nd bounce) reaching the different areas of visual fields and space.

Figure 25 presents the chosen BSDF files of the two roller shades that were eventually tested with the proposed methodology of this thesis.

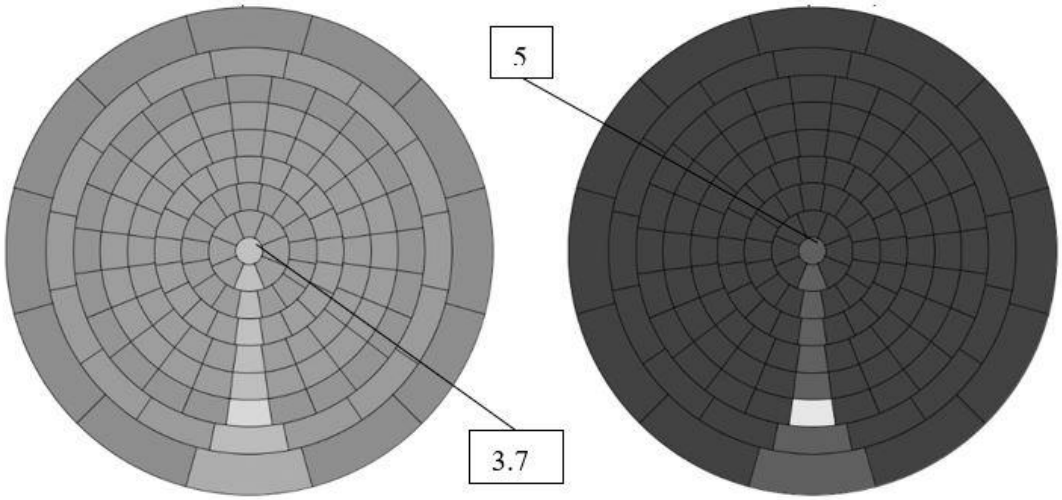

Figure 25: The tested BSDF files as presented by the BSDFviewer.

LUND UNIVERSITY

Dept of Architecture and Built Environment: Division of Energy and Building Design
Dept of Building and Environmental Technology: Divisions of Building Physics and Building Services